Late Cambrian adakitic granite at Kinchina Quarry: Implications for the evolution of the Delamerian Orogen

Thesis submitted in accordance with the requirements of the University of Adelaide for an Honours Degree in Geology/Geophysics

Christian Mark George
November 2018

THE UNIVERSITY of ADELAIDE

Abstract

The Monarto Granite is exposed as 0.2-3 metre sills at the Kinchina Quarry west of Murray Bridge. These medium-fine grained granite sheets intrude migmatite formed from Early Cambrian Kanmantoo Group turbidites and are interleaved with meta-dolerite sills of similar thickness. These granites and mafic sills appear to be synchronous with the late stages of Delamerian folding and metamorphism and the granite was dated at 495.4 ± 0.6 Ma using U-Pb on monazite. Kinchina granite sills have geochemical features that make them unique amongst other Delamerian granites. They are peralumious, with very low Y (<10ppm) and with high Sr/Y ratios and with steep, LREE-enriched and HREE-depleted rare earth patterns without any Eu anomalies. Their geochemical characteristics clearly define them as silica-rich adakites. With initial εNd values of +1 -+2, similar to the interleaved mafic sills (εNd +2-+3) these granites have the most primitive (mantle-like) isotopic compositions of all the Delamerian granites. The composition of the Kinchina meta-dolerites is consistent with a MORB-like parent melt contaminated by about 5-8% continental crust.

Geochemical modelling demonstrates that these adakite melts can form by partial melting of mafic rocks with compositions exactly the same as those of their near contemporary Kinchina sills (including their crustal contamination). Modelling is best matched by ~20% melting in the plagioclase-absent, garnet –CPX-rutile stable field. This eclogite facies melting must occur at pressures > 1.4GPa (> 50 Km depth) and ~980^{o}C. These are upper mantle pressures and suggest the crustal-contaminated mafic parents were partially melted following delamination from the lower crust.

There is good evidence that the Delamerian orogeny was terminated by a latest Cambrian phase of rapid uplift, exhumation and erosion, prior to the post-tectonic (480± 5 Ma) phase of voluminous A-

type magmatism. The evidence provided by the timing and petrogenesis of the Kinchina adakites strongly supports the suspicion that this terminal Delamerian exhumation was driven by delamination of dense, mafic crustal underplate.

Keywords

Adakite, Delamerian Orogeny, geochemistry, partial melting, eclogite, Kinchina, Sr, Y, delamination

TABLE OF CONTENTS

List of Figures, Images and Tables

Figures

Images

Tables

INTRODUCTION

This research project will investigate the origin and characteristics of a unique granite type rock which outcrops in Murray Bridge and more specifically the Kinchina Quarry. This unique granite is believed to be an adakite, if this is found to be correct it means it could have only formed under a specific set of tectonic regimes. This area is host to a large range of Delamerian granites, however the unique granite like rock or Adakite has unique characteristics and clear differences to the surrounding granites. Adakites are a granite like volcanic rocks with a specific geochemical signature (Table 1) they're classified mainly by high Sr and low Y. Adakites are the result of high pressure melting with residuals of garnet and sometimes amphiboles. Due to adakites being categorised by certain parameters it can become difficult to know whether or not they are in fact adakites or adakite like rocks. These parameters being their geochemical characteristics defined above and the setting in which they're formed. Defant and Drummond (Defant & Drummond, 1990) explain that adakites can only form at arcs above subduction zones and ensure that this is what separates adakites from "adakite-like" rocks. While a number of sources agree with this, a large number also state that adakites can form in a number of different tectonic regimes:

- Normal asthenosphere-derived arc magmas by upper plate crustal interaction and fractional crystallisation and do not require slab melting.(Richards & Kerrich, 2007)
- The result of tear off of a subducting slab and the exposure of a "slab window" to the mantle
- Due to mafic under-plate delamination under eclogite facies

Throughout the literature a number of different regimes are explored but one thing is solid; Adakites do form from partial melting of the subducting slab or melting of a mafic source. Throughout this paper, two types of adakite petrogenesis theories will be explored; the result of tear off of a subducting slab and the exposure of a "slab window" to the mantle or due to mafic under-plate delamination.

Table 1: Main geochemical features of adakite (Castillo, 2006)

Characteristics	**Possible links to subducted slab melting**
High SiO_2 (≥56 wt%)	High Pressure melting of eclogite/garnet amphibolite
High Al_2O_3 (≥15 wt%)	At ~ 70 wt % SiO_2: high P partial melting of eclogite or amphibolite
Low MgO (< 3 wt%)	And low Ni and Cr; if primary melt, not derived from a mantle peridotite
High Sr (>300 ppm)	Melting of plagioclase or absence of plagioclase in residue
No Eu anomaly	Either minor plagioclase residue or source basalt depleted in Eu
Low Y (< 15 ppm)	Mean low HREE; indicative of garnet as a residual or liquidus phase
High Sr/Y (>20)	Higher than that produced by normal crystal fractionation; indicative of garnet and amphibole as a residual phase or liquidus phase
Low Yb (<1.9 ppm)	Meaning low HREE: indicative of garnet as a residual or liquidus phase
High La/Yb (>20)	LREE enriched relative to HREE; indicative of garnet as a residual or liquidus phase

The term and classification of adakite was first suggested by Defant and Drummond (1990) who determined that they have SiO2 ≥56 wt percent, Al2O3 ≥15 wt percent, MgO normally <3 wt percent, Mg number ≈0.5, Sr ≥400 ppm, Y ≤18 ppm, Yb ≤1.9 ppm, Ni ≥20 ppm, Cr ≥30 ppm, Sr/Y ≥20, La/Yb ≥20, and 87Sr/86Sr ≤0.7045. Adakites (Defant and Drummond 1990)(Moyen, 2009)(Richards 2007) are believed to be the result of relatively high pressure partial melting of mafic source rocks in equilibrium with clinopyroxene and garnet or hornblende and in the absence of plagioclase.

(Richards & Kerrich, 2007) They are typically associated with subduction and partial melting of hot and young slabs(Macpherson, Dreher, & Thirlwall, 2006) (Qian & Hermann, 2013; Richards & Kerrich, 2007). Conditions for melting of mafic rocks in the slab are often correlated with the development of slab tears or slab break-off. Adakite may also be due to melting of delaminated mafic keels from the base of the overlying plate.

The distinctive conditions of adakite formation are highlighted by key geochemical features (Table 1) including their high Sr and low Y signatures and typically fractionated REE patterns with low HREE and without negative Eu anomalies. These features indicate the formation of these magmas in equilibrium with garnet or amphibole residues. Some adakites are relatively enriched in magnesium, possibly due to interaction between the slab-derived melt and peridotite of the mantle wedge (Cox, Foden, & Collins, 2018) Two potential theories will be discussed throughout this paper, it is suggested that one of these is responsible for the adakites located in Kinchina.

A range of theories have been suggested for adakite petrogenesis (Castillo, 2006) however only two (as mentioned earlier) appear to fit the required criteria at Murray Bridge and its relationship to the Delamerian Orogeny. One model suggests mafic under-plate delamination involving delamination and partial melting as the mafic rocks at the base of the crust descend into the underlying mantle. This foundering crust was converted to eclogite prior to delaminate into the mantle, and melting of this garnet-rich lithology is interpreted to be responsible for the adakite magmas. (Qian & Hermann, 2013)

Alternatively adakite may be the result of tear off of the Delamerian subducting slab and the exposure of a "slab window" to the up flow of hot asthenosphere. These gaps expose the eclogite facies mafic rocks of the upper part of the subducting slab to high temperatures creating the heat and pressure required to accumulate Adakitic signature magmas (Thorkelson & Breitsprecher, 2005) Both of these theories require a subducting slab, meaning these adakites would have had to have formed when the slab was subducting below this margin. As well as this, both theories require garnet or amphibole as residual minerals. As the granitoid rocks at Kinchina are believed to have Adakitic compositions, this paper will explore which of the two models is most appropriate and what the implications for the evolution of subduction beneath the SE Gondwanan margin in the Late Cambrian. The Monarto adakite differs from the other Delamerian granites and most likely originated by high pressure melting in the presence of residual garnet, a desirable setting being 10-12.5kbar and 800-900 degrees Celsius and 15kbar and 800 degrees Celsius (Qian & Hermann, 2013). These adakites formed from two possible tectonic regimes; the result of tear off of the Delamerian subducting slab and the exposure of a "slab window" at the end of the Delamerian or due to mafic under-plate delamination also at the end of the Delamerian Orogeny.

This study aims to confirm the Monarto granite is adakite like in composition, while simultaneously determining the absolute age of the "adakite" and its surrounding stratigraphy. Establishing the age of the geology in the Murray Bridge Quarry or Kinchina will enable us to determine the structural history of the area as well as its relationship and timing with the Delamerian Orogeny. Further understanding subduction related tectonics and magmatism in the formation of Eastern Australia and

Delamerian Orogeny is vital; the source of the adakite will be determined and whether or not it formed via the tear-off theory or the mafic under-plate delamination theory.

In the Middle Cambrian in South Eastern Australia, the Orogeny caused by the contraction and convergence of the Pacific and the Australian plate is known as the Delamerian Orogeny (Figure 1). This Orogenic belt extends across Antarctica as the Ross Orogen (Foden, Elburg, Dougherty-Page, & Burtt, 2006) The development of the Delamerian-Ross Orogeny represented the initiation of the Orogenic (subduction) character of the Pacific margin of Gondwana; the start of the "Terra Australis" of Cawood (2005) and continued to the present day (New Zealand). This westward subduction with its the fundamental driving factors (ridge-push and slab roll-back) was responsible for the Andean-style Orogeny. The South Australian part of the Delamerian Orogen is composed of predominantly Neoproterozic and Early Cambrian sediments (JD Foden et al., 2002) these areas are known as the Adelaidean, Normanville and Kanmantoo groups (JD Foden et al., 2002; John Foden et al., 2002) as well as mafic suites. The area of focus within this project is the Murray Bridge quarry at Kinchina (west of Murray Bridge) which is composed of Kanmantoo Group sedimentary rocks metamorphosed to migmatite grade intruded by sheets or sill of mafic and granitoid rocks. The mafic rocks are now hornblende-plagioclase amphibolites while the medium grained granites have distinctive compositions tentatively identifying them as adakites. Adakite production is interpreted as due to high pressure partial melting of mafic source rocks with eclogite (garnet-clinopyroxene) mineralogy. Adakite production is often correlated with melting either of mafic parts of the subducting oceanic slab or due to delamination of underplated mafic keels to the upper plate (Qian & Hermann, 2013)

The generation and timing of adakite may represent an important factor in the understanding of the Delamerian Orogeny and associated subduction. This will be investigated throughout this thesis.

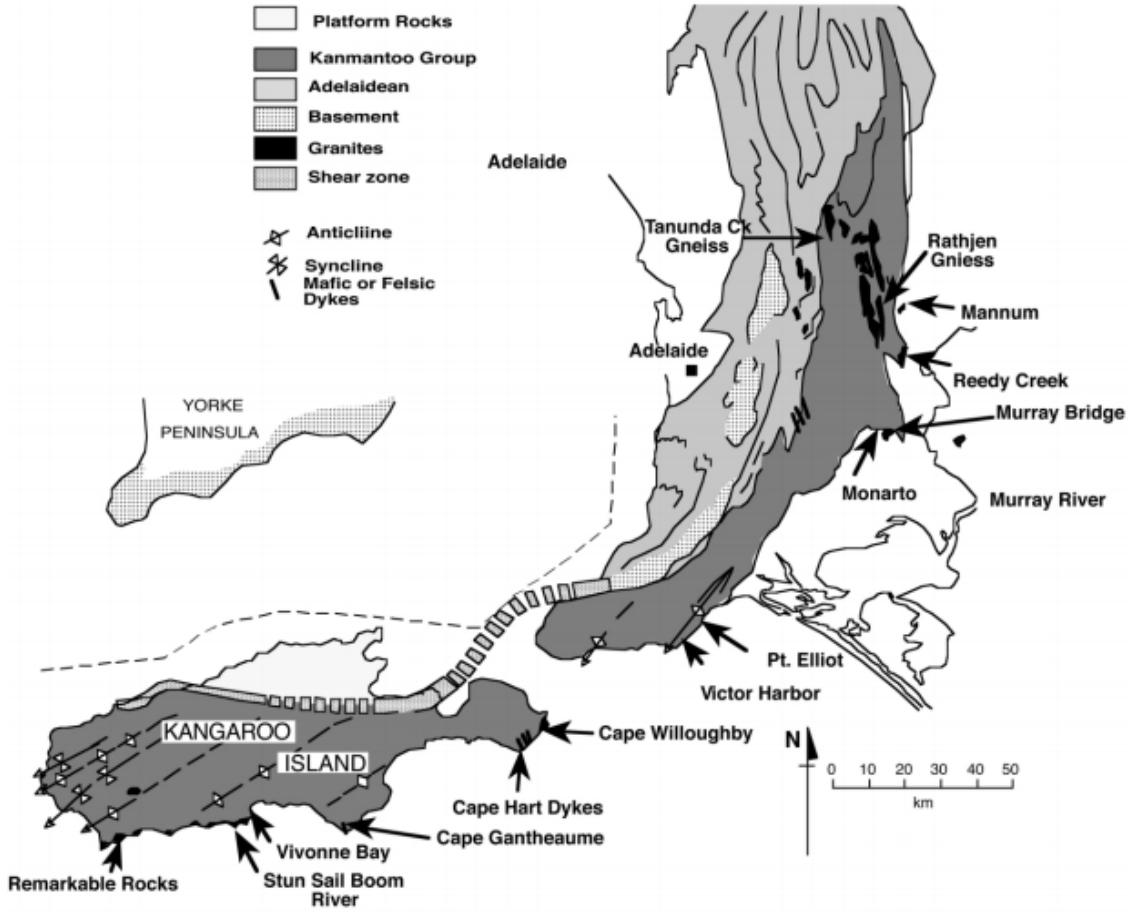

Figure 1: Geology of the Southern Adelaide Fold Belt (Delamerian Orogen) (Foden 2006)

The initiation of the Delamerian Orogeny is believed to have occurred at 514Ma in the mid Cambrian (Foden et al., 2006) which in turn initiated deformation and metamorphism. This Orogeny was thought to have been driven by the start of subduction in the western Pacific. It has been speculated that the new slab may have reached the transition zone (650km) about 24 million after subduction commenced, initiating slab roll-back at about 490 Ma. (Foden et al., 2006) Once slab roll-back had begun, convergent deformation of the Australian margin ceased, terminating the Delamerian Orogeny. The end of convergent deformation was marked by the change

from syn-orogenic I- and S-type granite magmatism to post-tectonic A-type granite intrusion (Foden et al., 2006; JD Foden et al., 2002) The termination of the Delamerian may also have been the result of slab tear-off with subsequent outboard (eastward) stepping of subduction. The slab tear-off or roll-back would have caused the mobilization and influx of hot asthenosphere leading to the production of the post-tectonic, high temperature A-type granite magmatism together with lithospheric extension (JD Foden et al., 2002)

The reorganization and assemblage of Gondwana is said to be responsible for the Delamerian Orogeny, the stress being transferred from these collisions supposed to have initiated it.(Boger & Miller, 2004; Foden et al., 2006) Tectonically, the Delamerian Orogeny is driven by subduction along the margin of Gondwana; this subduction is responsible for the lithospheric extension and slab roll-back which created the increase in geotherm and ultimately magmatism. The simultaneous increase in both the geotherm and magmatism is responsible for the regional deformation throughout the area.

METHODS

Fieldwork and Sampling:

31 samples were collected from the Kinchina Quarry in Murray Bridge, these samples were collected after examining the face of the quarry wall and determining which lithologies were most important to the project. Using a geological hammer and chisel, rock samples roughly the size of a bowling ball were removed from the face of the rock wall. Once they had been placed on the ground and lined up to give each sample a name

and number they were broken up with a sledge hammer if required, then taken back to storage at The University of Adelaide.

Geochemistry:

20 samples were taken to the rock crushing laboratory to be turned into rock flour for geochemistry purposes. Each sample went through the same steps in order to be turned into rock flour. Firstly, weathered material is removed from the rock in order to keep the integrity of the samples chemistry. Then, the whole rock sample is crushed in the jaw crusher and turned into a gravel like mass, depending on the size of the pieces in the gravel the sample may or may not have to be placed through a smaller crushing machine. Once the gravel was the appropriate size, this flour was placed into a tungsten carbide mill head and further crushed into a flour; appropriate to be sent off to the lab to assess the geochemistry. These steps were repeated for each sample.

Thin sections:

2 samples (cg-18-3 and cg-18-11) were cut down between 5-10cm cube shape pieces and sent to Adelaide Petrography to be made into unpolished thin sections.

High Resolution 3D mapping and imaging:

In order to grasp a better understanding of the structural history and sequence of lithologies at the Murray Bridge quarry, high resolution 3D mapping and imaging was used. A range of advanced cameras as well as a drone were used to capture the area; using motion (SfM) photogrammetry a 3D model was produced as well as aerial images collected by a DJI Inspire UAV with a Zenmuse X3 camera. Pix4D was the program used to process said images. Using AutoPano Giga Stitch softwar deep zoom images

were produces by merging multiple images with 30% horizontal and vertical overlap: These were captured using a Gigapan Pro system paired with a Lumix DMC-FZ2500 digital camera.

Isotopes:

To evenly represent the mafic, migmatite and adakitic suites from Murray Bridge; six samples were chosen for Nd-Sm-Sr radiogenic isotope analysis as well as two standards and a blank. One pegmatite, one migmatite, two mafics and two adakites were all analysed at The University of Adelaide under David Bruce's supervision. In preparation samples were spiked with 150Sm/147Nd. After this they were to be broken down by three critical acids (Hydrochloric, Nitric and Hydrofluoric), 2mL 15M HNO3 and 4mL 28M hydrofluoric acid were placed into each Teflon vial and Teflon bomb. Samples which contained zircons were placed in bombs and sent to the oven in metal jackets to be heated for 4-5 days at 200 degrees Celsius to be evaporated. The Teflon vials however were placed on a hotplate at 140 degrees Celsius and evaporated to dry, with refills of Hydrofluoric acid and Nitric acid accordingly. After all samples were evaporated 6M hydrochloric acid was added to all samples; bombs placed in oven for a further 2 days. Using column chromatography, the total of ten samples were placed through the columns in order to extract Sr, Nd and Sm.

U-Pb Dating of Zircons:

A singular sample from the field was chosen to resemble an even spread of the adakitic rock suite and marked to be used for zircons, to determine the age of the suite. Once the sample was taken back to the university it was crushed into a fine gravel and the zircon sized grains were separated in a X, repeating the process of crushing the pieces too large

to move through the X. Once a sufficient amount of the appropriate sized grains is acquired, this rock flour is taken into the pan and separated using water. Repeat this panning method until a sufficient amount of "zircons" are available. Separate the water from the sediments by drying out the sediments, once dried used a magnet to remove all magnetic material and dry the remaining on a hot plate. Take the remaining minerals to the microscope and pick 80-100 zircons with a needle placing the zircons onto the epoxy mount. Once picked, cover epoxy in resin and let cool for roughly 24 hours. Once the mount is dry the zircons need to be exposed; using the sandpaper and the diamond sander to polish the mount. Repeat the sanding process until all grains are exposed, as well as polishing to get a clean finish. After these steps the mount is taken to Adelaide Microscopy to be carbon coated and prepared for the laser.

These "zircons" after close examination under the CL were found to be monazites and after repeating the method in an attempt to find zircons, monazites were picked again. Due to this and time constraints the monazites were used to determine the age of the adakite suite. Like the zircons, U-Pb isotopes were analysed at Adelaide Microscopy, University of Adelaide in the monazites using an ASI RESOlution ArF excimer laser ablation system with a S155 large format sample chamber. Coupled with an Agilent 7900x ICP-MS. Using a spot size of 19 micron a repetition rate of 5 Hz with a fluence at the sample of ~2 J/cm2, samples were ablated. In a Helium atmosphere, with Ar carrier gas for movement to the ICP-MS. Each analysis had 30 seconds gas background with no laser fire, followed by 30 seconds of ablated signal.

MADEL (207/206 Age 491Ma, 206/238 Age 515Ma, 207/232 Age 510Ma) was the primary standard, secondary standards were monazites 222 (450 Ma) and Anbat (~525 Ma). Isotopes measured included: 29Si, 31P, 43Ca, 89Y, 139La, 140Ce, 141Pr, 146Nd, 147Sm, 157Gd, 202Hg, 204Pb, 206Pb, 207Pb, 208Pb, 232Th, and 238U.

OBSERVATIONS AND RESULTS

Geology

The Kinchina Quarry located in Murray Bridge plays host to a unique set of rock types, regionally being placed within the Delamerian Orogeny and ultimately surrounded by different Delamerian and Monarto granites. The Quarry itself hosts a number of lithology's including: the Kanmantoo migmatite, the Kinchina mafic suite, the unique granite like adakite being the main focus of this project amongst a range of different pegmatites. Sequentially the mafic was deposited first followed by the migmatite and finally the adakite. The area shows a wide range of textures and different mineralogical characteristics:

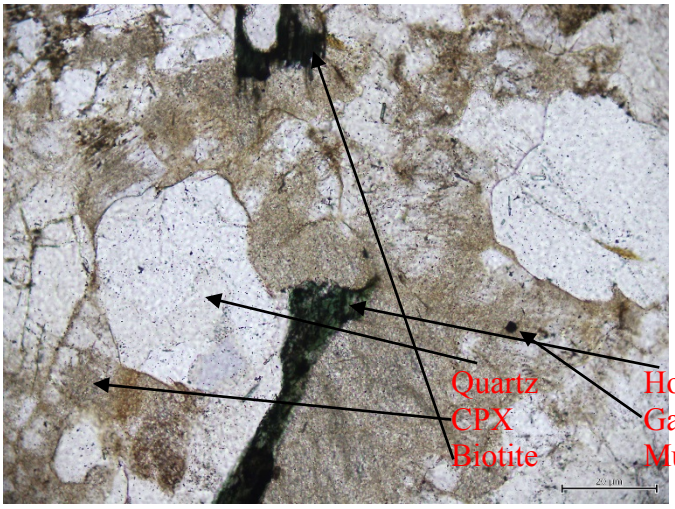

Image 1: CG-18-3 (adakite) in PPL

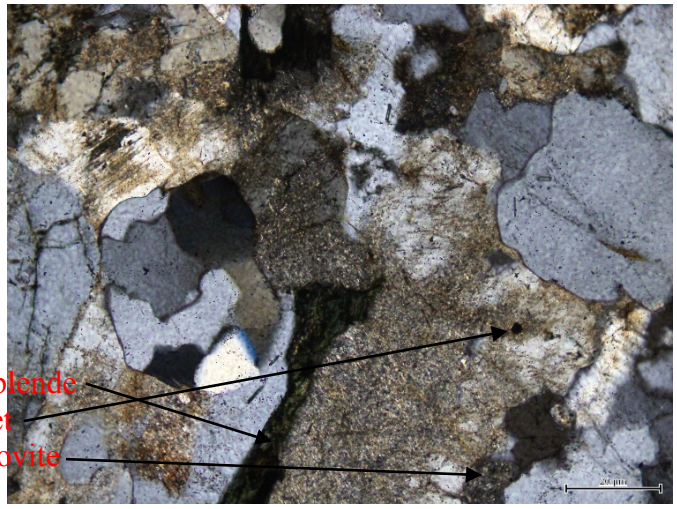

Image 2: CG-18-3 (adakite) in XPL

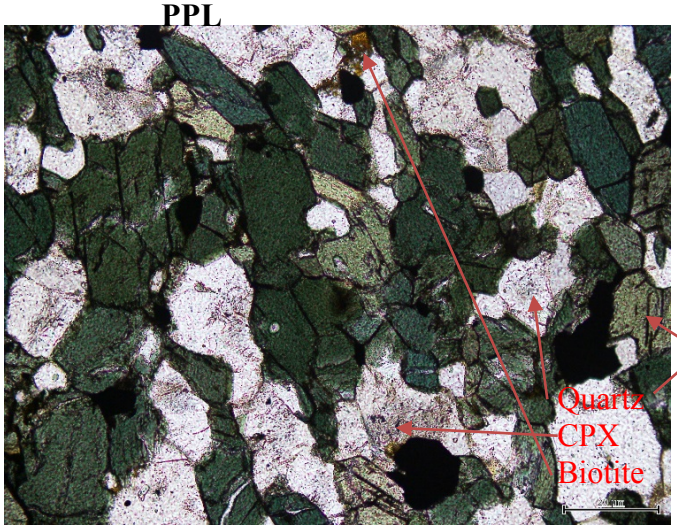

Image 3: CG-18-11 (mafic) in PPL

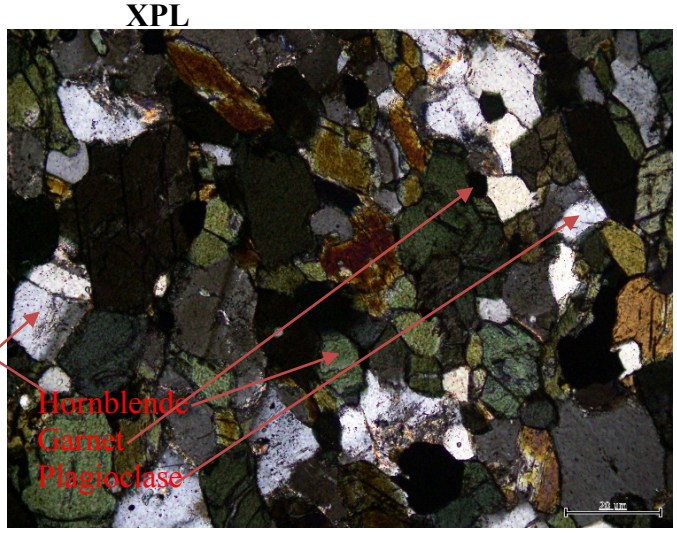

Image 4: CG-18-11 (mafic) in XPL

Images 1-4 have been taken from thin sections produced by an adakite and a mafic sample from Kinchina. CG-18-3 is the adakite while the mafic is CG-18-11; the adakites contain a large ground mass of equant and subhedral quartz. Amongst this are fine to medium grained hornblende (Amphibole) ranging from tabular to bladed grains. Fine grained isotropic garnet is throughout ranging from 1-5% of the assemblage. Other minerals include: Clinopyroxene, biotite and muscovite all ranging between fine and medium grains. The mafics are thoroughly enriched with fine to medium grained amphibole and fine to medium grained quartz making up the matrix. Much like the adakite the mafic also contains medium grains of biotite, fine to medium grained clinopyroxene and a small percentage < 10% of equant, subhedral garnet. As well as these, medium grained equant to columnar plagioclase is throughout the assemblage which contains inclusions of clinopyroxene indicating clinopyroxene formed before this. Kinchina Quarry roughly 7 kilometres to the west of Murray Bridge is a large (300 metres x 300 metres) open cut quarry. This quarry exposes three main lithologies: the adakite, the mafic suite or basalt and finally the Kanmantoo migmatite.

- Adakite: The adakites are fine to medium grained granites which have distinctive compositions tentatively identifying them as adakites. The mineral composition under hand lens include: fine grains of quartz, biotite, amphibole and plagioclase with potential for other minerals too fine to see. The thickness of the beds vary in size from a 10-20 centimetres up to 5 metres. The adakite cross cut both the mafic and the migmatite indicating it was late in the deposition of the outcrop.

- Mafic: The mafic rocks are now hornblende-plagioclase amphibolites which under hand lens show fine to medium grains of plagioclase surrounded by a fine matrix of amphiboles as well as biotite and other minerals too fine to identify. Like the adakite have sills varying in size from a few centimetres to 3 metres in width. The mafic or metadolerite sills cross cut the migmatite but don't cross cut the adakite indicating it was second in the depositional sequence.

- Kanmantoo migmatite: complexly deformed sequence of Kanmantoo Group sedimentary rocks metamorphosed to migmatite grade. The migmatite shows distinctive layering which can sometimes be disrupted by leucosomes, the mineralogy includes an array of fine grained almost stretched minerals indicating metamorphism. Minerals include: a wealth of biotite and muscovite, plagioclase, K-feldpsar, quartz which can all range from fine to coarse grained in the leucosomes. The migmatite is intruded by sheets or sills of mafic and granitoid rocks and leucosomes found throughout and like both the adakite and mafic can vary in structural thickness (10-20 centimetres up to 4-5 metres)

Mapping and Field Observations

Image 5a: Southern face of Kinchina Quarry (25 metres side to side)

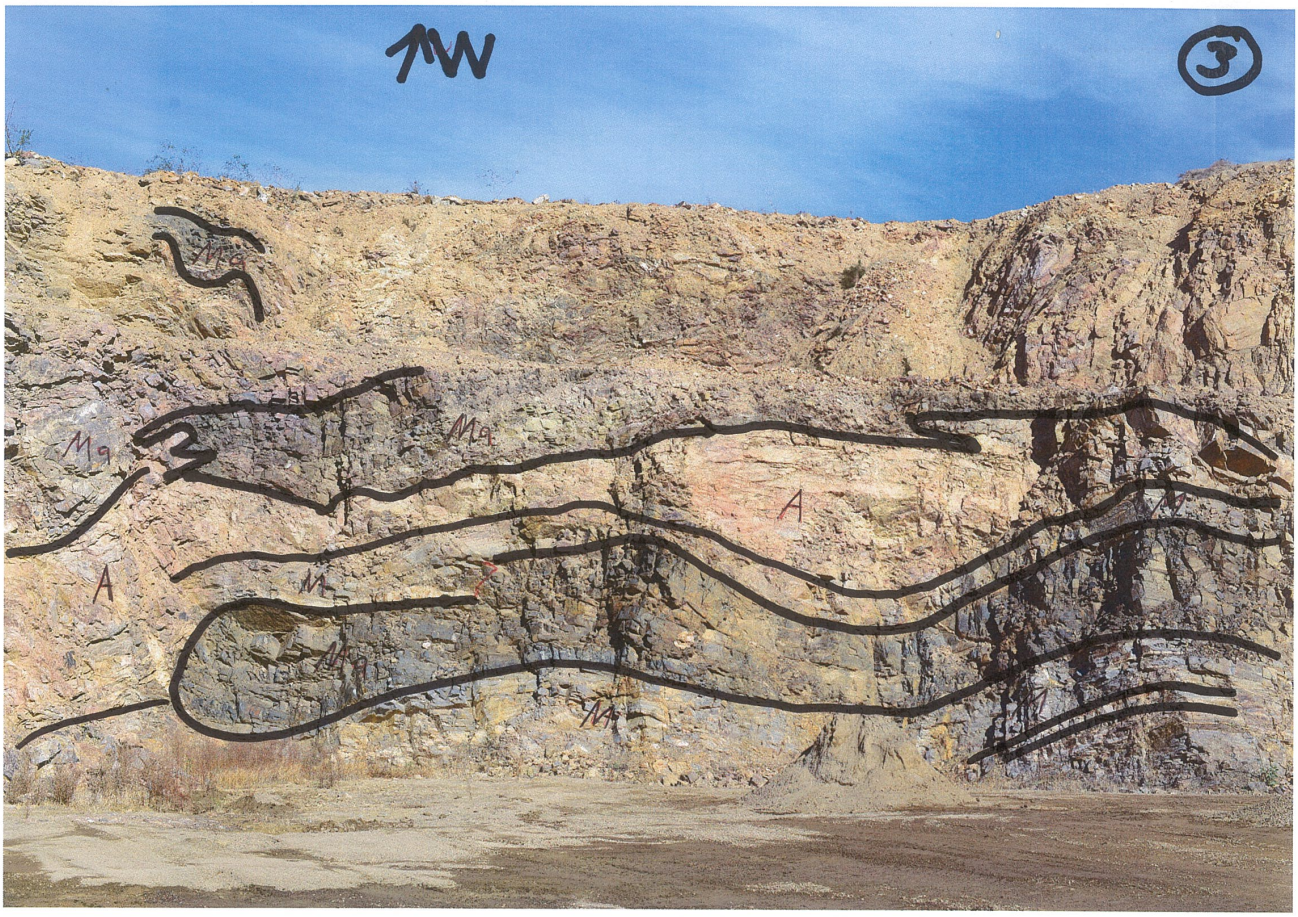

Image 5b: Western face of Kinchina Quarry (25 metres side to side)

Image 5c: Northern face of Kinchina Quarry (25 metres side to side)

Image 5d: North-western face of Kinchina Quarry (25 metres side to side)

Observing the site at Kinchina in Murray Bridge there are three prevailing lithologies: The adakite, the mafic sills and thirdly the migmatite. A few indicators can be noted in determining the timing of each event. Firstly, the adakite intrudes upon both the mafic and the migmatite in several places across the site, for example image 3 shows a large separation between the migmatite layers as well as the mafic sills; this separation is caused by the adakite. It cross cuts the migmatite layering indicating it is syntectonic to late in the sequence. The migmatite also intrudes upon the mafic sills making the sills the oldest in the sequence. These sills show strong alignments of amphiboles indicating a tectonic fabric while the predominant deformation is found throughout the entire

sequence the adakite is only slightly deformed again supporting the idea that it is late in the sequence.

Image 5e: Birdseye view of Murray Bridge Quarry displaying the mapped quarry faces

Geochronology

Table 2: U-Pb Analyses taken from Monazites from Kinchina (Concordance is either above (>100) or below (<100) Concordia)

Analysis	207Pb/235U		206Pb/238U		rho	Concordance	207Pb/206Pb		206Pb/238U	
MBQ_1	0.618	0.012	0.08061	0.00091	0.1856	144.2039	0.0559	0.0012	0.08061	0.00091
MBQ_2	0.654	0.018	0.07984	0.00098	0.16242	133.7353	0.0597	0.0017	0.07984	0.00098
MBQ_3	0.617	0.014	0.07932	0.00081	0.2631	140.6383	0.0564	0.0012	0.07932	0.00081
MBQ_4	0.628	0.014	0.07925	0.00079	0.22514	138.0662	0.0574	0.0013	0.07925	0.00079
MBQ_5	0.631	0.015	0.08097	0.0009	0.3043	142.5528	0.0568	0.0013	0.08097	0.0009
MBQ_7	0.63	0.016	0.08041	0.00082	0.41105	141.5669	0.0568	0.0013	0.08041	0.00082
MBQ_8	0.622	0.011	0.07869	0.00082	0.13753	136.6146	0.0576	0.0011	0.07869	0.00082
MBQ_9	0.631	0.011	0.07938	0.00086	0.47115	137.5737	0.0577	0.001	0.07938	0.00086
MBQ_10	0.638	0.017	0.0788	0.0011	0.29063	136.3322	0.0578	0.0015	0.0788	0.0011
MBQ_11	0.62	0.013	0.07977	0.00077	0.088711	141.4362	0.0564	0.0013	0.07977	0.00077
MBQ_12	0.661	0.013	0.08107	0.00076	0.44701	137.1743	0.0591	0.001	0.08107	0.00076
MBQ_13	0.6253	0.0097	0.0792	0.00074	0.20012	138.9717	0.05699	0.00093	0.0792	0.00074
MBQ_14	0.6322	0.0098	0.0799	0.00077	0.074255	140.669	0.0568	0.0011	0.0799	0.00077
MBQ_15	0.632	0.012	0.07953	0.00079	0.031132	138.0729	0.0576	0.0012	0.07953	0.00079
MBQ_16	0.63	0.013	0.08023	0.00082	0.19215	140.2622	0.0572	0.0013	0.08023	0.00082
MBQ_17	0.629	0.014	0.07897	0.0008	0.24468	138.0594	0.0572	0.0013	0.07897	0.0008
MBQ_18	0.626	0.01	0.0795	0.0008	0.15705	139.2294	0.0571	0.0011	0.0795	0.0008
MBQ_19	0.637	0.015	0.0801	0.00096	0.36202	138.5813	0.0578	0.0013	0.0801	0.00096
MBQ_20	0.63	0.012	0.08018	0.00083	0.0892	141.6608	0.0566	0.001	0.08018	0.00083
MBQ_21	0.631	0.012	0.07941	0.00081	0.24906	139.8063	0.0568	0.0011	0.07941	0.00081
MBQ_22	0.635	0.015	0.08071	0.00082	0.0986	141.8453	0.0569	0.0014	0.08071	0.00082
MBQ_23	0.639	0.015	0.08032	0.00078	0.38558	139.2028	0.0577	0.0012	0.08032	0.00078
MBQ_24	0.64	0.014	0.08005	0.00084	0.17808	138.0172	0.058	0.0013	0.08005	0.00084
MBQ_25	0.622	0.014	0.08041	0.00093	0.28485	143.5893	0.056	0.0012	0.08041	0.00093
MBQ_26	0.633	0.011	0.07989	0.00068	0.25403	139.4241	0.0573	0.001	0.07989	0.00068
MBQ_27	0.627	0.011	0.07986	0.00072	0.29443	140.8466	0.0567	0.0011	0.07986	0.00072
MBQ_28	0.629	0.013	0.07969	0.00082	0.12157	139.807	0.057	0.0012	0.07969	0.00082
MBQ_29	0.624	0.014	0.08103	0.00099	0.27725	143.9254	0.0563	0.0013	0.08103	0.00099
MBQ_30	0.63	0.012	0.07986	0.0008	0.22864	141.0954	0.0566	0.0011	0.07986	0.0008
MBQ_31	0.631	0.012	0.07997	0.00085	0.37446	140.0525	0.0571	0.0011	0.07997	0.00085
MBQ_32	0.627	0.012	0.07995	0.00073	0.090727	139.5288	0.0573	0.0012	0.07995	0.00073
MBQ_33	0.627	0.01	0.08083	0.00069	0.018791	142.5573	0.0567	0.001	0.08083	0.00069
MBQ_34	0.62	0.023	0.07829	0.00091	0.25722	135.4498	0.0578	0.0019	0.07829	0.00091
MBQ_35	0.631	0.013	0.08023	0.00081	0.50144	141.7491	0.0566	0.001	0.08023	0.00081
MBQ_36	0.634	0.02	0.0793	0.0017	0.037757	134.635	0.0589	0.0017	0.0793	0.0017
MBQ_37	0.621	0.012	0.07831	0.00091	0.46068	136.1913	0.0575	0.0012	0.07831	0.00091
MBQ_38	0.622	0.014	0.07941	0.00067	0.25479	140.0529	0.0567	0.0013	0.07941	0.00067
MBQ_39	0.641	0.014	0.08087	0.00077	0.18374	140.3993	0.0576	0.0012	0.08087	0.00077

MBQ_40	0.723	0.032	0.0806	0.0012	0.29123	123.6196	0.0652	0.0025	0.0806	0.0012
MBQ_41	0.639	0.014	0.08126	0.00088	0.074206	142.812	0.0569	0.0012	0.08126	0.00088
MBQ_42	0.642	0.015	0.0809	0.00099	0.13133	139.7237	0.0579	0.0015	0.0809	0.00099
MBQ_43	0.974	0.039	0.0791	0.0013	-0.19715	88.18283	0.0897	0.0041	0.0791	0.0013
MBQ_44	0.635	0.013	0.07911	0.00093	0.29733	136.8685	0.0578	0.0011	0.07911	0.00093
MBQ_45	0.63	0.014	0.07934	0.00078	0.33483	140.6738	0.0564	0.0012	0.07934	0.00078
MBQ_46	0.645	0.013	0.07981	0.00082	0.18272	137.3666	0.0581	0.0011	0.07981	0.00082
MBQ_47	0.639	0.014	0.07989	0.00077	0.17691	137.9793	0.0579	0.0012	0.07989	0.00077
MBQ_48	0.645	0.013	0.07987	0.00095	0.35247	137.2337	0.0582	0.0011	0.07987	0.00095
MBQ_49	0.626	0.011	0.07983	0.00066	-0.01237	139.8074	0.0571	0.0011	0.07983	0.00066
MBQ_50	0.628	0.022	0.0795	0.0013	0.22474	134.7458	0.059	0.0024	0.0795	0.0013
MBQ_51	0.63	0.013	0.07954	0.00076	0.221	137.851	0.0577	0.0012	0.07954	0.00076
MBQ_52	0.635	0.013	0.08034	0.00087	0.14283	140.9474	0.057	0.0013	0.08034	0.00087
MBQ_53	0.624	0.013	0.07986	0.00083	0.18316	142.0996	0.0562	0.0011	0.07986	0.00083
MBQ_54	0.642	0.016	0.07955	0.00099	0.39122	137.6298	0.0578	0.0013	0.07955	0.00099
MBQ_55	0.63	0.012	0.07976	0.00081	0.02331	140.1757	0.0569	0.0012	0.07976	0.00081
MBQ_56	0.6401	0.0093	0.08102	0.00088	0.051692	140.8554	0.05752	0.00098	0.08102	0.00088
MBQ_57	0.635	0.012	0.07984	0.00076	0.23304	139.8249	0.0571	0.0011	0.07984	0.00076
MBQ_58	0.614	0.013	0.07975	0.00071	0.043672	142.4107	0.056	0.0012	0.07975	0.00071
MBQ_59	0.616	0.014	0.07769	0.0008	0.36878	135.113	0.0575	0.0012	0.07769	0.0008
MBQ_60	0.619	0.012	0.07958	0.00073	0.075565	141.6014	0.0562	0.0011	0.07958	0.00073
MBQ_61	0.628	0.012	0.0783	0.00089	0.20502	134.3053	0.0583	0.0012	0.0783	0.00089
MBQ_62	0.631	0.015	0.07923	0.00084	0.19823	139.2443	0.0569	0.0013	0.07923	0.00084
MBQ_63	0.604	0.014	0.079	0.00073	0.26103	142.5993	0.0554	0.0013	0.079	0.00073
MBQ_64	1.029	0.098	0.0838	0.0017	0.63467	93.11111	0.09	0.0072	0.0838	0.0017

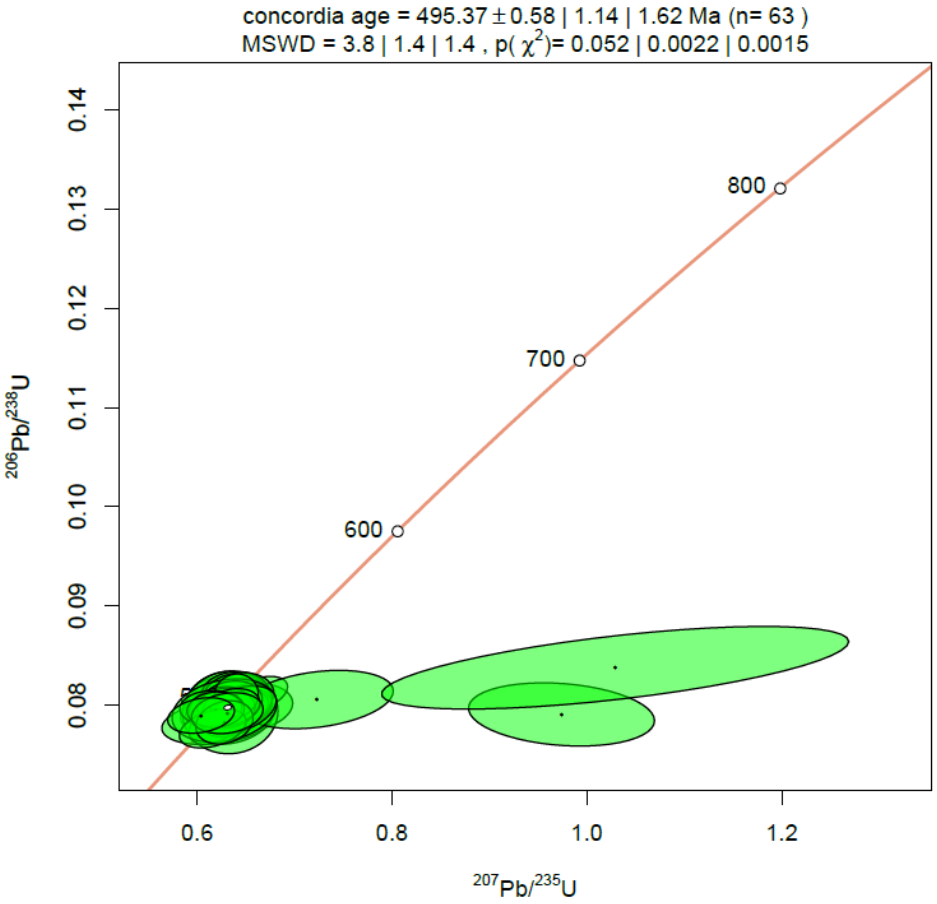

Figure 2a: U-Pb Monazite dating Concordia

Figure 1a shows the ages for the monazites used under the Adelaide Microscopy using ASI RESOlution ArF excimer laser ablation system. The age was determined to be 495.37±0.58, this age supports the idea that the adakite was syntectonic to late in formation in regards to the Orogeny of the Delamerian. Figure 1b shows the adakite in comparison to surrounding delamerian granites (the adakite is in red), this again supports the syntectonic to late theory. Table 1 summarises all age data.

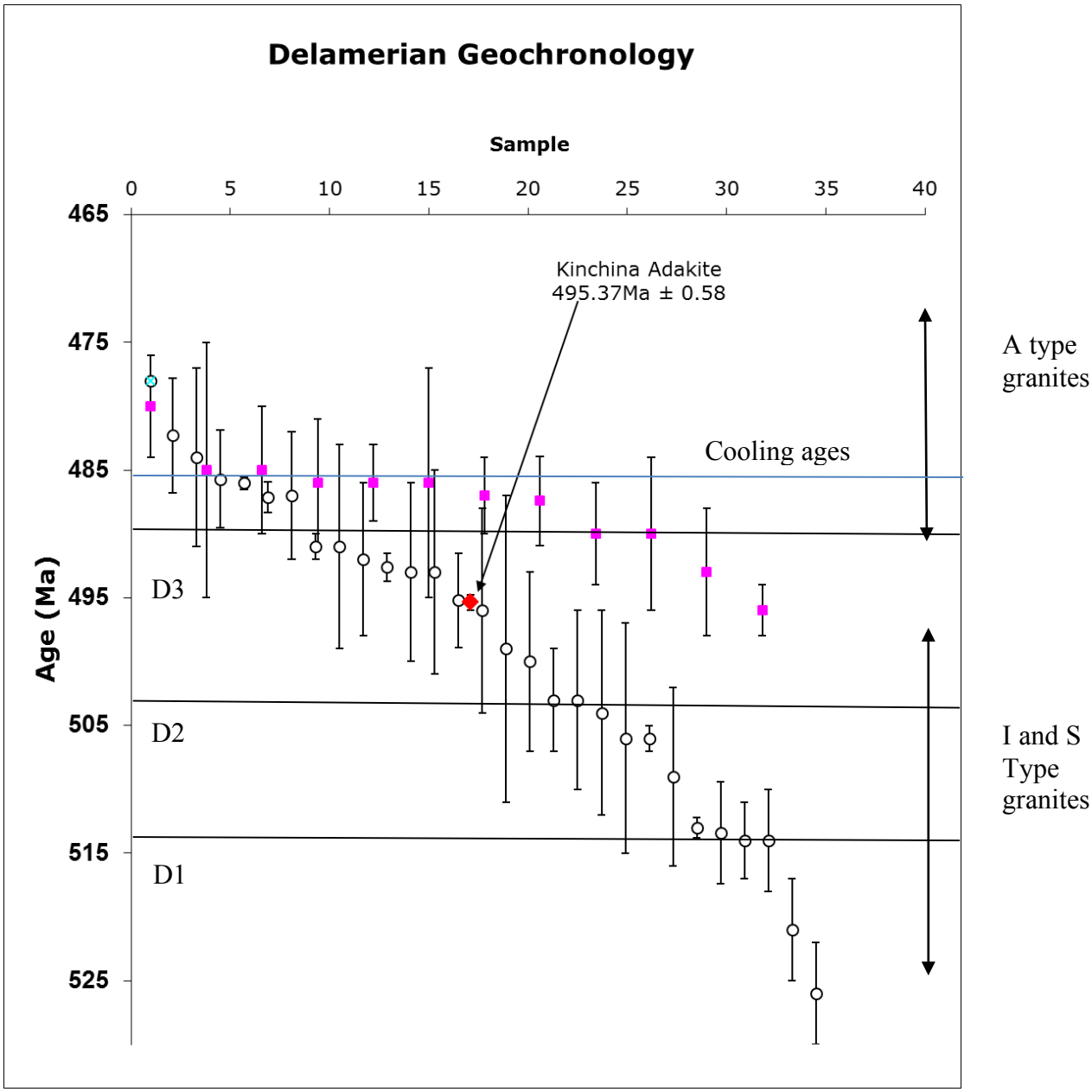

Figure 2b Delamerian Geochronology taken from J Foden including the adakite Monazite date in red with Deformation stages (D1, D2, D3), Granite types and formation stages and cooling ages

Table 3: Summary of Age of adakite

Sample	Rock Type	N	MSWD	U-Pb Age (Ma)	2σ
CG-18-6	Adakite	63	1.4	495.37	1.14

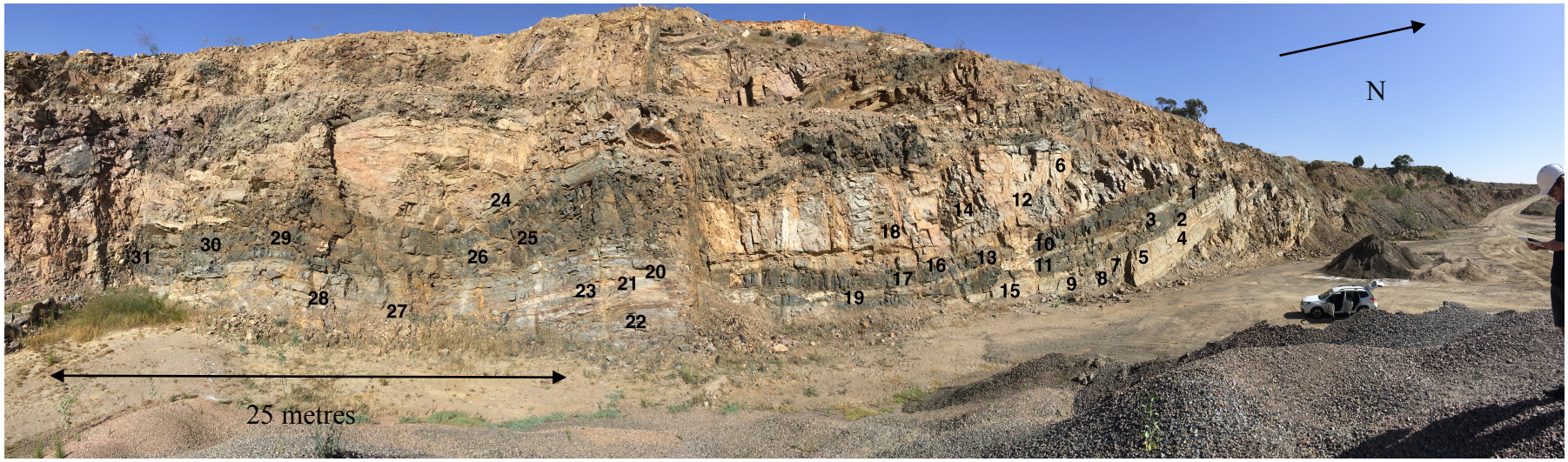

Image 6: Face map including numbered locations of samples in Kinchina Quarry, Murray Bridge

Table 4: Rock type, sample number and location of each sample taken from site

Sample	**CG-18-1**	**CG-18-2**	**CG-18-3**	**CG-18-4**	**CG-18-5**	**CG-18-6**	**CG-18-7**
Location	1	2	3	4	5	6	7
Rock Type	Adakite	Adakite	Adakite	Mig Leucosome	Migmatite	Adakite	Migmatite
Sample	**CG-18-8**	**CG-18-9**	**CG-18-10**	**CG-18-11**	**CG-18-12**	**CG-18-13**	**CG-18-14**
Location	8	9	10	11	12	13	14
Rock Type	Mig Leucosome	Migmatite	Mafic	Mafic	Adakite	Mafic	Adakite
Sample	**CG-18-15**	**CG-18-16**	**CG-18-17**	**CG-18-18**	**CG-18-19**	**CG-18-20**	**CG-18-21**
Location	15	16	17	18	19	20	21

Rock Type	Migmatite	Mafic	Mafic	Adakite	Mig Leucosome	Migmatite	Adakite layer in Mig
Samples	**CG-18-22**	**CG-18-23**	**CG-18-24**	**CG-18-25**	**CG-18-26**	**CG-18-27**	**CG-18-28**
Location	22	23	24	25	26	27	28
Rock Type	Migmatite	Adakite	Adakite	Mafic	Mafic	Mig Leucosome	Mig Leucosome
Sample	**CG-18-29**	**CG-18-30**	**CG-18-31**				
Location	29	30	31				
Rock Type	Mafic	Mafic	Pegmatite				

Geochemistry

Table 5: Major elements of the Kinchina samples with the mafics in blue, Migmatites in green and adakites highlighted in orange. While the white are classified as being unclassified or a pegmatite.

Sample	CG 18 11	CG 18 13	CG 18 25	CG 18 26	CG 18 29	CG 18 16	CG 18 17	CG 18 1	CG 18 12	CG 18 6	CG 18 6 Rpt
Rock type	Mafic	Mafic	Mafic	Mafic	Mafic	Mafic	Mafic	Adakite	Adakite	Adakite	Adakite
Locality	11	13	25	26	29	16	17	1	12	6	6
SiO2	49.27	49.35	49.38	50.55	51.02	51.24	51.50	70.08	71.62	71.82	71.86
TiO2	2.59	2.60	1.90	1.91	1.97	2.08	1.72	0.31	0.26	0.25	0.26
Al2O3	13.50	13.50	14.20	14.30	14.20	14.00	14.50	15.50	15.10	15.10	15.10
Fe2O3	14.84	14.51	14.05	13.31	12.81	13.78	12.92	2.19	1.97	2.09	2.09
MnO	0.26	0.24	0.29	0.20	0.20	0.20	0.20	0.02	0.02	0.02	0.02
MgO	6.16	6.10	6.89	6.55	6.01	5.71	6.57	0.66	0.52	0.52	0.53
CaO	8.45	8.54	8.87	8.52	8.96	7.56	8.59	0.69	1.91	1.79	1.79
Na2O	2.39	2.35	2.31	2.37	2.37	2.37	2.76	4.13	4.27	4.13	4.17
K2O	0.78	0.86	1.14	0.71	0.87	1.27	0.64	4.49	3.42	3.34	3.34
P2O5	0.35	0.34	0.22	0.25	0.27	0.29	0.14	0.22	0.09	0.08	0.08
S	0.10	0.08	0.02	0.07	0.10	0.00	0.02	<0.001	0.02	0.02	0.02
LOI	0.61	0.71	0.74	0.61	0.63	0.82	0.54	0.97	0.28	0.29	0.30
Total	99.30	99.18	100.00	99.34	99.40	99.32	100.10	99.25	99.48	99.45	99.56
Mg#	0.45	0.45	0.49	0.49	0.48	0.45	0.50	0.37	0.34	0.33	0.33
Sr	240.00	220.00	220.00	220.00	230.00	200.00	230.00	220.00	580.00	570.00	570.00
Zr (wt %)	0.03	0.03	0.02	0.02	0.03	0.02	0.02	0.02	0.03	0.03	0.03
Zr	280.00	270.00	170.00	200.00	270.00	240.00	160.00	150.00	320.00	280.00	280.00
Ba (wt %)			0.01		0.00	0.01	0.00	0.24	0.23	0.23	0.24
Ba			80.00		40.00	70.00	30.00	2410.00	2280.00	2340.00	2360.00
V (wt%)	0.04	0.04	0.04	0.03	0.03	0.04	0.03	0.00		0.00	0.00
V	440.00	440.00	380.00	340.00	320.00	370.00	320.00	30.00		20.00	40.00
Cl	0.08	0.07	0.08	0.08	0.09	0.07	0.06	0.03	0.03	0.03	0.03
Co	58.00	59.00	56.00	55.00	54.00	54.00	55.00	69.00	72.00	60.00	56.00
Cr	130.00	130.00	130.00	180.00	160.00	160.00	220.00	20.00	<10	<10	<10
Cs	0.10	0.20	2.30	0.60	1.30	1.10	0.20	0.90	0.70	0.80	0.80
Cu	75.00	277.00	10.00	130.00	220.00	121.00	47.00	6.00	5.00	4.00	3.00
Ga	24.00	23.00	23.80	21.80	20.60	22.40	21.40	18.80	18.40	19.20	17.80
Hf	2.40	3.20	1.20	4.20	2.00	5.60	2.80	2.40	6.40	3.20	3.20

Li	<10	<10	<10	<10	<10	<10	<10	<10	<10	<10	<10
Nb	11.00	11.00	8.00	9.50	11.50	10.50	11.00	10.00	10.00	8.00	7.50
Ni	50.00	46.00	54.00	54.00	44.00	50.00	52.00	8.00	<2	<2	<2
Pb	2.00	3.00	4.00	2.00	3.00	3.00	3.00	8.00	14.00	15.00	15.00
Rb	20.60	24.00	64.80	24.80	36.80	43.80	16.20	138.00	79.80	83.00	82.80
Sc	39.00	40.00	39.00	37.00	37.00	34.00	37.00	4.00	2.00	2.00	2.00
Sn	2.60	2.50	6.50	4.00	2.50	4.10	3.50	3.50	1.00	1.00	0.80
Ta	0.60	0.50	0.50	0.60	0.70	0.50	0.70	0.60	0.30	0.20	<0.1
Th	3.10	3.80	3.10	3.90	4.30	6.60	2.80	33.20	63.80	66.90	60.60
Tl	0.10	0.10	0.40	0.10	0.30	0.20	<0.1	0.80	0.30	0.30	0.30
U	0.70	1.10	0.60	1.10	1.40	1.40	1.10	2.50	3.30	3.30	3.20
Y	50.40	48.90	42.80	43.00	42.80	50.50	41.80	10.90	4.70	4.70	4.60
Zn	76.00	74.00	84.00	54.00	70.00	62.00	56.00	16.00	24.00	28.00	28.00
La	13.40	12.40	8.60	9.10	10.90	11.70	10.50	79.90	124.00	129.00	115.00
Ce	35.50	30.40	22.60	25.90	29.30	28.00	27.90	129.00	181.00	183.00	169.00
Pr	5.15	4.40	3.50	3.95	4.35	4.50	4.10	12.00	15.00	15.30	13.70
Nd	26.00	22.50	18.50	20.60	22.80	23.90	21.30	39.20	42.70	44.80	39.80
Sm	7.75	6.90	5.75	6.55	6.70	7.45	6.65	5.75	4.45	4.70	4.30
Eu	2.25	1.90	1.80	1.90	2.00	2.15	2.10	1.35	1.05	1.10	1.05
Gd	8.80	8.20	6.80	7.40	7.40	8.80	7.40	3.60	2.20	2.40	2.20
Tb	1.54	1.42	1.22	1.26	1.26	1.46	1.28	0.48	0.24	0.24	0.22
Dy	9.75	8.95	8.05	7.90	8.40	9.60	8.10	2.40	1.05	1.10	0.90
Ho	2.08	2.02	1.74	1.76	1.78	2.10	1.76	0.48	0.18	0.18	0.20
Er	5.95	5.70	4.95	4.95	5.00	5.95	4.75	1.20	0.50	0.50	0.50
Tm	0.80	0.80	0.70	0.70	0.70	0.80	0.70	0.15	0.05	0.05	0.10
Yb	5.45	5.25	4.40	4.40	4.55	5.35	4.55	1.15	0.55	0.50	0.50
Lu	0.78	0.74	0.64	0.64	0.64	0.78	0.68	0.16	0.08	0.08	0.08

Sample	CG 18 14	CG 18 18	CG 18 2	CG 18 3	CG 18 24	CG 18 31	CG 18 21	CG 18 28	CG 18 4	CG 18 8
Rock type	Adakite	Adakite	Adakite	Adakite	Adakite	Migmatite	Migmatite	Migmatite	Migmatite	Migmatite
Locality	14	18	2	3	24	31	21	28	4	8
SiO2	71.94	72.67	72.76	72.83	73.12	74.22	74.35	75.39	75.57	76.0
TiO2	0.26	0.22	0.21	0.22	0.28	0.06	0.21	0.17	0.11	0.1
Al2O3	15.10	14.80	14.60	14.70	14.40	15.40	14.30	14.30	14.70	14.1
Fe2O3	1.94	1.69	1.77	2.19	1.62	0.40	1.69	1.20	0.83	1.0
MnO	0.02	0.02	0.02	0.04	0.02	<0.01	0.02	0.01	0.01	0.0
MgO	0.53	0.44	0.43	0.61	0.57	0.19	0.53	0.49	0.35	0.3
CaO	1.85	1.72	1.45	0.39	1.69	1.04	1.41	0.66	1.45	1.8
Na2O	4.08	4.37	4.41	4.05	4.73	7.36	5.23	6.51	6.02	5.3
K2O	3.72	3.02	3.11	4.07	2.35	0.65	1.86	0.92	0.77	0.5
P2O5	0.10	0.12	0.07	0.07	0.07	0.11	0.06	0.14	0.07	0.0
S	0.01	0.00	0.00	0.00	0.00	0.00	0.01	0.00	0.00	0.0
LOI	0.29	0.34	0.46	0.99	0.47	0.26	0.40	0.43	0.41	0.3
Total	99.84	99.41	99.29	100.16	99.32	99.70	100.07	100.22	100.29	99.7
Mg#	0.35	0.34	0.32	0.36	0.41	0.48	0.38	0.45	0.46	0.4
Sr	560.00	520.00	450.00	230.00	500.00	230.00	350.00	110.00	360.00	290.0
Zr (wt %)	0.03	0.02	0.01	0.02	0.03	0.01	0.02	0.01	0.01	0.0
Zr	270.00	180.00	130.00	190.00	280.00	90.00	210.00	70.00	110.00	120.0
Ba (wt %)	0.27	0.23	0.21	0.19	0.16	0.03	0.09	0.02	0.02	0.0
Ba	2690.00	2250.00	2080.00	1940.00	1600.00	270.00	920.00	190.00	230.00	220.0
V (wt %)	0.00	0.00		0.00	0.00	0.00	0.00	0.00	0.00	0.0
V	30.00	30.00		30.00	20.00	20.00	30.00	20.00	30.00	30.0
Cl	0.03	0.03	0.02	0.02	0.03	0.03	0.03	0.03	0.03	0.0
Co	92.00	67.00	77.00	56.00	68.00	98.00	62.00	100.00	95.00	74.0
Cr	<10	<10	<10	<10	<10	<10	<10	<10	<10	<10
Cs	0.70	0.70	0.70	0.70	1.00	0.80	0.90	2.20	0.90	0.4
Cu	16.00	18.00	2.00	3.00	7.00	2.00	2.00	3.00	3.00	2.0
Ga	18.00	16.60	18.00	18.20	18.20	16.00	18.20	16.60	17.00	16.0
Hf	6.00	4.40	5.00	5.00	6.20	0.20	3.60	1.60	1.20	2.2
Li	<10	<10	<10	<10	<10	<10	<10	<10	<10	<10
Nb	7.00	13.50	9.00	6.50	9.50	3.50	10.00	5.50	3.00	2.0
Ni	<2	<2	<2	<2	<2	<2	<2	<2	<2	4.0
Pb	15.00	13.00	15.00	8.00	17.00	7.00	12.00	5.00	8.00	8.0
Rb	84.20	70.40	76.60	133.00	61.00	25.00	56.40	57.40	37.00	21.0
Sc	2.00	2.00	2.00	2.00	2.00	1.00	3.00	3.00	2.00	2.0

Sn	0.90	0.90	1.30	1.30	1.30	1.90	1.70	2.60	2.00	0.8(
Ta	0.20	0.50	0.50	0.30	0.30	0.30	0.50	0.80	0.20	0.2(
Th	55.10	43.00	43.30	40.10	64.10	6.00	37.00	10.40	13.50	13.8(
Tl	0.30	0.30	0.50	0.50	0.30	0.10	0.30	0.20	0.20	0.1(
U	2.80	2.70	2.90	2.80	3.40	0.70	3.00	1.60	1.20	1.7(
Y	4.90	6.40	6.20	6.10	5.70	7.90	6.20	7.00	3.20	5.2(
Zn	24.00	18.00	12.00	12.00	24.00	10.00	12.00	12.00	18.00	12.0(
La	122.00	82.90	85.70	82.30	65.50	9.00	56.30	22.70	23.70	25.7(
Ce	172.00	123.00	128.00	123.00	99.80	16.70	89.40	40.40	40.10	43.7(
Pr	14.10	10.30	11.20	10.90	8.70	1.85	8.20	4.50	3.90	4.3(
Nd	41.40	30.90	33.00	32.50	26.30	6.90	25.90	17.40	13.30	15.0(
Sm	4.15	3.60	3.95	3.95	3.35	1.50	3.65	3.05	2.10	2.5(
Eu	1.10	1.00	1.00	1.00	0.90	0.50	0.80	0.60	0.60	0.8(
Gd	2.00	2.00	2.20	2.40	2.00	1.20	2.20	2.20	1.20	1.8(
Tb	0.22	0.24	0.24	0.26	0.22	0.20	0.32	0.30	0.16	0.2(
Dy	1.05	1.40	1.30	1.30	1.20	1.30	1.55	1.55	0.80	1.1(
Ho	0.20	0.26	0.24	0.24	0.22	0.30	0.28	0.28	0.12	0.2(
Er	0.55	0.75	0.70	0.65	0.65	0.90	0.55	0.70	0.35	0.6(
Tm	0.10	0.10	0.10	0.10	0.10	0.15	0.05	0.10	<0.05	0.0(
Yb	0.50	0.70	0.70	0.70	0.75	0.85	0.50	0.70	0.35	0.5(
Lu	0.08	0.10	0.10	0.12	0.12	0.12	0.06	0.10	0.04	0.08

Sample	**CG 18 19**	**CG 18 30**	**CG 18 5**	**CG 18 10**	**CG 18 9**
Rock type	Migmatite	Migmatite	Migmatite	Migmatite	Migmatite
Locality	19	30	5	10	9
SiO2	77.06	68.67	72.63	73.19	73.73
TiO2	0.02	0.82	0.55	0.53	0.52
Al2O3	14.10	13.00	12.10	12.00	11.40
Fe2O3	0.26	6.22	5.52	4.65	4.66
MnO	0.01	0.03	0.03	0.03	0.04
MgO	0.16	2.16	1.29	1.50	1.21
CaO	2.58	0.94	0.43	1.20	0.57
Na2O	4.86	3.99	1.46	4.26	2.24
K2O	0.49	2.60	4.54	1.55	4.25
P2O5	0.07	0.26	0.19	0.22	0.18
S	<0.001	0.01	0.00	0.01	0.00
LOI	0.36	0.57	0.97	0.42	0.67
Total	99.97	99.27	99.71	99.56	99.48
Mg#	0.55	0.41	0.32	0.39	0.34

Sr	280.00	170.00	130.00	250.00	160.00
Zr (wt %)	0.00	0.06	0.03	0.04	0.04
Zr	10.00	600.00	310.00	360.00	360.00
Ba (wt %)	0.01	0.04	0.11	0.05	0.11
Ba	130.00	420.00	1070.00	540.00	1130.00
V (wt %)	0.00	0.01	0.01	0.01	0.01
V	20.00	80.00	70.00	80.00	70.00
Cl	0.02	0.05	0.03	0.04	0.03
Co	54.00	52.00	54.00	44.00	48.00
Cr	<10	70.00	70.00	50.00	50.00
Cs	0.70	3.20	2.00	2.00	1.10
Cu	4.00	4.00	3.00	8.00	6.00
Ga	14.40	20.20	16.60	17.80	16.80
Hf	<0.2	5.60	3.20	4.00	4.00
Li	<10	20.00	10.00	10.00	10.00
Nb	<0.5	17.50	7.00	11.50	10.50
Ni	<2	32.00	18.00	20.00	20.00
Pb	6.00	7.00	8.00	7.00	13.00
Rb	19.40	118.00	162.00	69.80	120.00
Sc	<1	12.00	8.00	9.00	8.00
Sn	0.50	6.00	3.20	2.40	3.00
Ta	<0.1	1.40	0.40	0.80	0.70
Th	1.60	29.80	17.60	18.00	17.70
Tl	0.10	0.50	0.60	0.30	0.50
U	0.40	5.00	2.30	3.20	2.60
Y	2.30	23.80	12.50	17.90	19.80
Zn	10.00	20.00	12.00	16.00	24.00
La	4.30	92.80	46.00	57.30	49.20
Ce	7.00	180.00	86.90	115.00	101.00
Pr	0.75	19.90	9.80	12.80	11.60
Nd	2.95	76.80	37.00	48.60	44.30
Sm	0.65	13.60	6.90	8.80	8.60
Eu	0.50	2.00	1.20	1.30	1.55
Gd	0.60	9.00	4.60	6.20	6.20
Tb	0.08	1.20	0.64	0.80	0.92
Dy	0.50	5.80	2.90	4.35	4.60
Ho	0.08	1.00	0.52	0.80	0.86
Er	0.25	2.60	1.25	1.90	2.10
Tm	<0.05	0.35	0.15	0.25	0.25

Yb	0.25	1.95	0.95	1.65	1.70
Lu	0.02	0.24	0.14	0.22	0.24

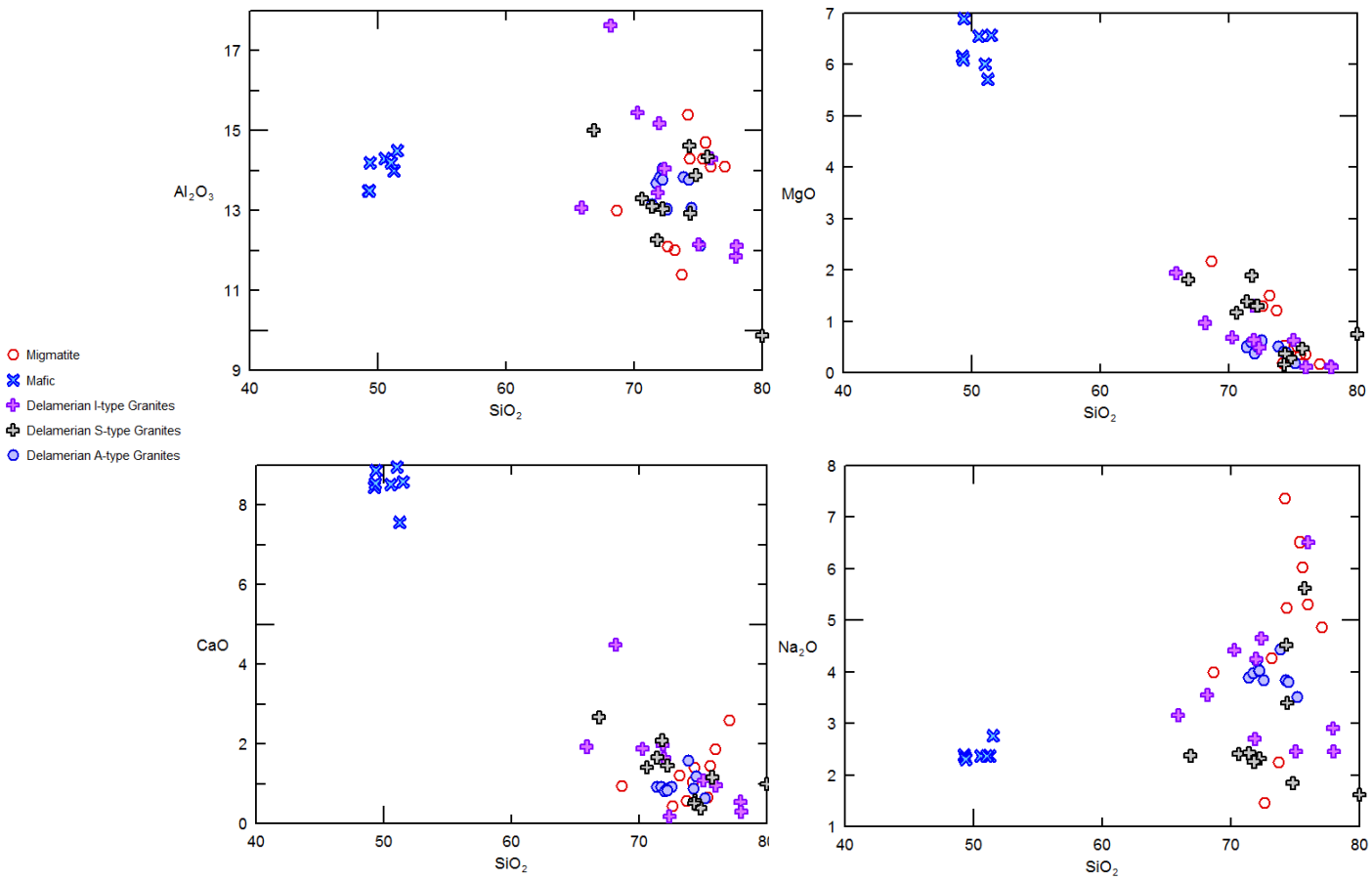

Figures 3a-3d: Different oxides plotted against SiO_2 for the Kinchina mafics and migmatites in comparison to the Delamerian granites (3a is Al_2O_3, 3b is MgO, 3c is CaO and finally 3d is Na_2O)

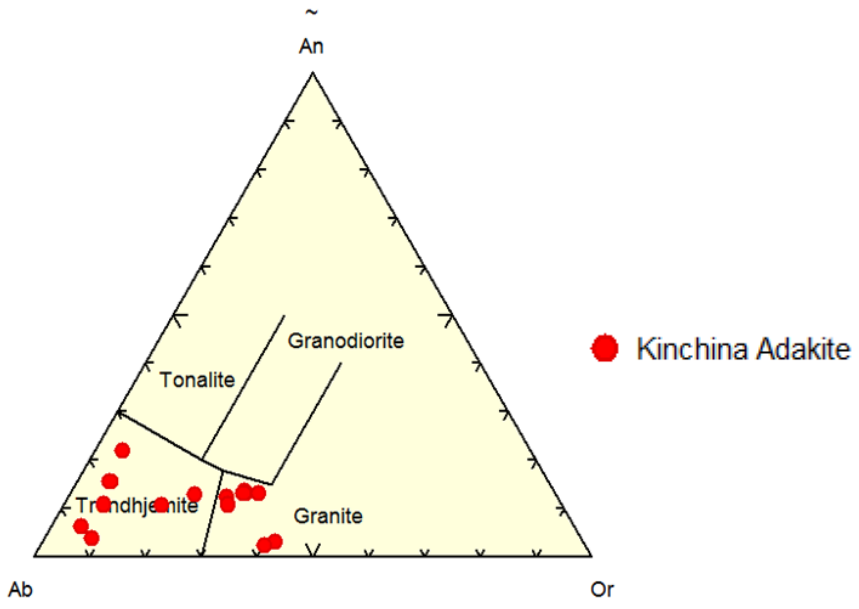

Figure 3e: Average adakites on a An-Ab-Or triangle plot to demonstrate the similarities and differences to Granites

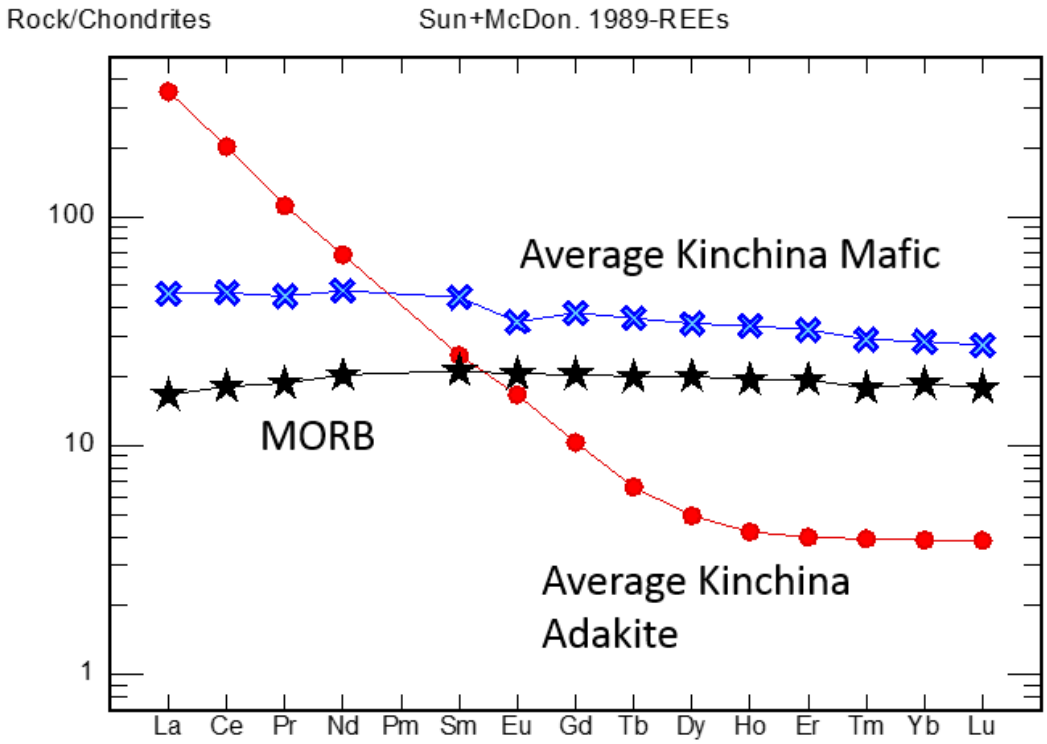

Figure 4: Kinchina averages for Adakites and Mafics compared to Mid Ocean Ridge Basalt (MORB)

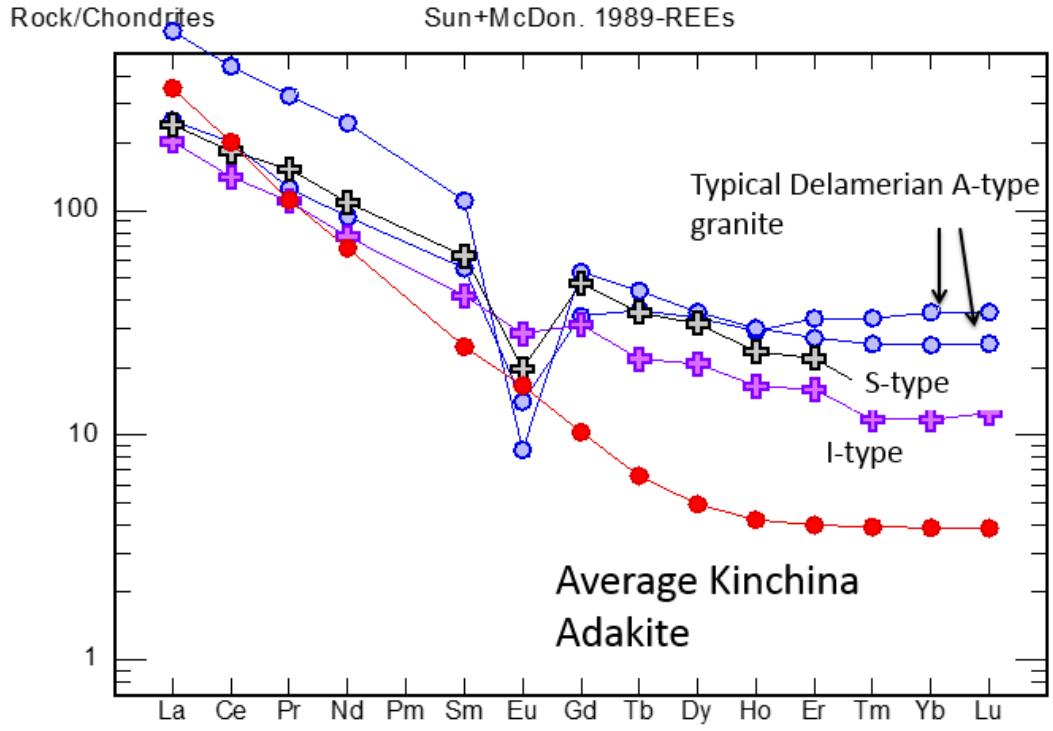

Figure 5: Kinchina average Adakites plotted against surrounding Delamerian granites.

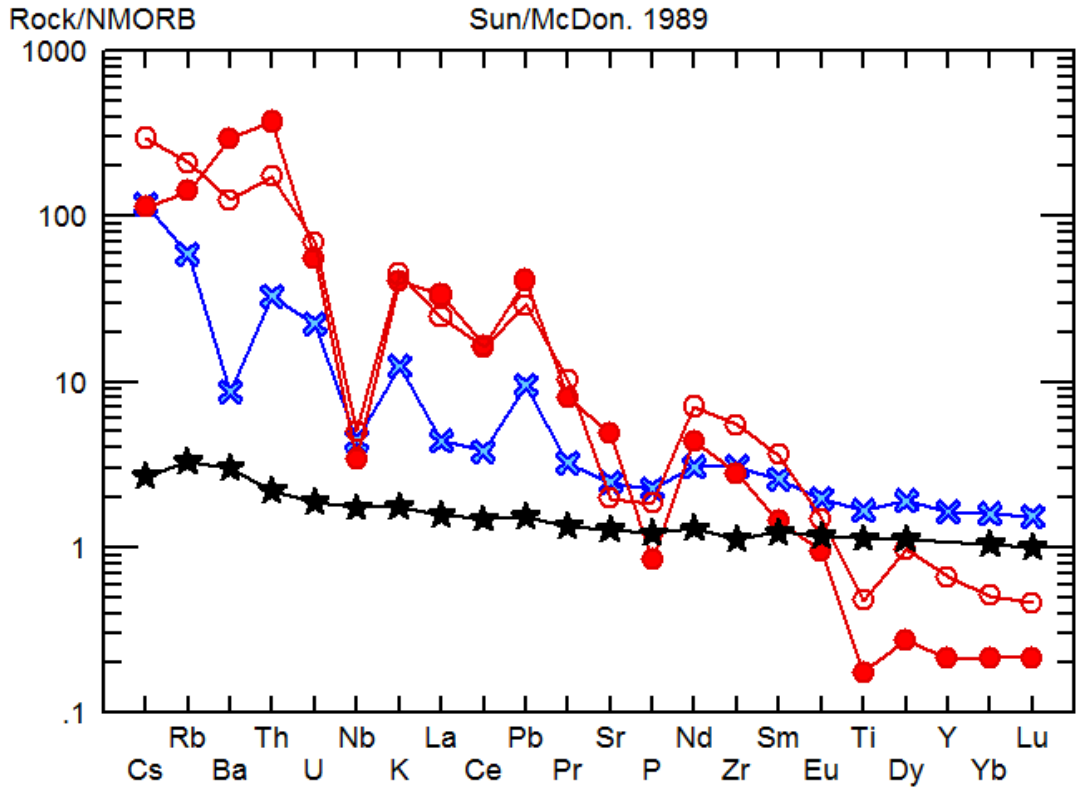

Figure 6: Spider plot of MORB (black star) against Kinchina average mafic (blue cross), Kinchina Migmatite (Clear red circle) and Kinchina adakite (Full red circle)

The lithology being focused on throughout this paper, the adakites as defined by Defant and Drummond (1990) have geochemical signatures close to "SiO2 ≥56 wt percent, Al2O3 ≥15 wt percent, MgO normally <3 wt percent, Mg number ≈0.5, Sr ≥400 ppm, Y ≤18 ppm" Comparing the geochemical signatures of the Kinchina rocks with known Adakitic data from around the world as well as known Delamerian granites (I, S and A types) allows the Kinchina adakites to be placed into a relevant category. Three Harker diagrams were produced (Figures 3a through to 3c) Al_2O_3 against SiO_2, MgO against SiO_2 and Sr against Y respectively. Arguably these elements are the most fundamental in determining an adakitic rock. Figure 1a shows the adakites plotting well within the known adakite fields with SiO_2 values well above 56% and Al_2O_3 fluctuating around

15% with the Delamerian granites showing mostly higher SiO_2. Figure 1b highlights the low MgO throughout the Kinchina adakites, known adakites and the Delamerian granites with high MgO values in the mafics. Again, the Kinchina adakites are well within the Magnesium signature of <3 wt percent. Thirdly, figure 1c compares Sr and Y; predominantly the Delamerian granites display quite high Y values this may be due to a lack in plagioclase meaning more Y in the melt. While the adakites and known adakites are all plotting above 300-400ppm Sr and almost all below 20ppm Y.

Secondly is the mafic suite, as this is a mafic suite it displays the typical peaks in both magnesium and iron (Table 5) (Figures 3a-3d) as well as this it shows high calcium in comparison to the surrounding migmatites and adakites. Its wealth in plagioclase classifies it as a mafic metadolerite.

The host rock, The Kanmantoo migmatite is part of a much larger (Kanmantoo group) metasandstone unit which spans for hundreds of kilometres ranging in different metamorphic rocks due to the deformation caused by the Delamerian Orogeny. These sediments were deposited rapidly to the east of Gondwana, after this burial ensued the Delamerian Orogeny and in turn activated metamorphism in the area. (Pawley, 2013) This metamorphism was triggered through three deformation stages (Figure 2b) which ultimately moved the grade between greenschist facies and upper amphibolite facies (Gum, 1998) It shows similarities between both the adakite and the mafic however the predominant features include high SiO_2, high Al_2O_3, low calcium, very low magnesium and high sodium. The migmatite shows great similarities with the mafic with drops and

peaks in trace element composition (Figure 6) notable peaks include potassium and lead with drops including barium and niobium.

Isotopes:

Table 6: Sm/Nd summary for samples from Kinchina

Sample	Age (Ma)	Sm (ppm)	Nd (ppm)	147Sm/144Nd	143Nd/144Nd	143Nd/144Nd(t)	2σ	eNd	eNd(t)	DM(t)
CG 18-6	495	4.080613	38.77	0.06363346	0.512086781	0.512086781	1.94E-06	-6.66249	1.88646	862.6407
CG 18-12	495	4.082746	37.49	0.065843268	0.512074779	0.512074779	6.22E-06	-6.75457	1.652045	880.2549
CG 18-19	495	0.497643	2.37	0.127174981	0.511506298	0.511506298	1.73E-06	-13.9017	-9.4513	2129.462
CG 18-11	495	6.889161	23.84	0.174717043	0.512118126	0.512118126	1.96E-06	1.088967	2.498676	1743.327
CG 18-5	495	6.878613	38.68	0.107513122	0.511299189	0.511299189	1.96E-06	-19.2056	-13.4965	2124.043
CG 18-29	495	5.74061	19.71	0.17604946	0.51217001	0.51217001	0.000116	2.186714	3.51206	1582.061

Table 6: Rb and Sr summary for samples from Kinchina

Sample	Age (Ma)	Rb (ppm)	Sr (ppm)	87Sr/88Sr	2σ	87Sr/88Sr(t)
CG 18-6	495	83	570	0.707200297	3.2584E-06	0.704180506
CG 18-12	495	79.8	580	0.70713997	2.90148E-06	0.70428668
CG 18-19	495	19.4	280	0.710440072	3.09276E-06	0.708659469
CG 18-11	495	20.6	240	0.711044928	2.52718E-06	0.707725549
CG 18-5	495	162	130	0.712974188	3.30331E-06	0.711536507

CG 18-29	495	36.8	230	0.753193245	3.429E-06	0.727233823

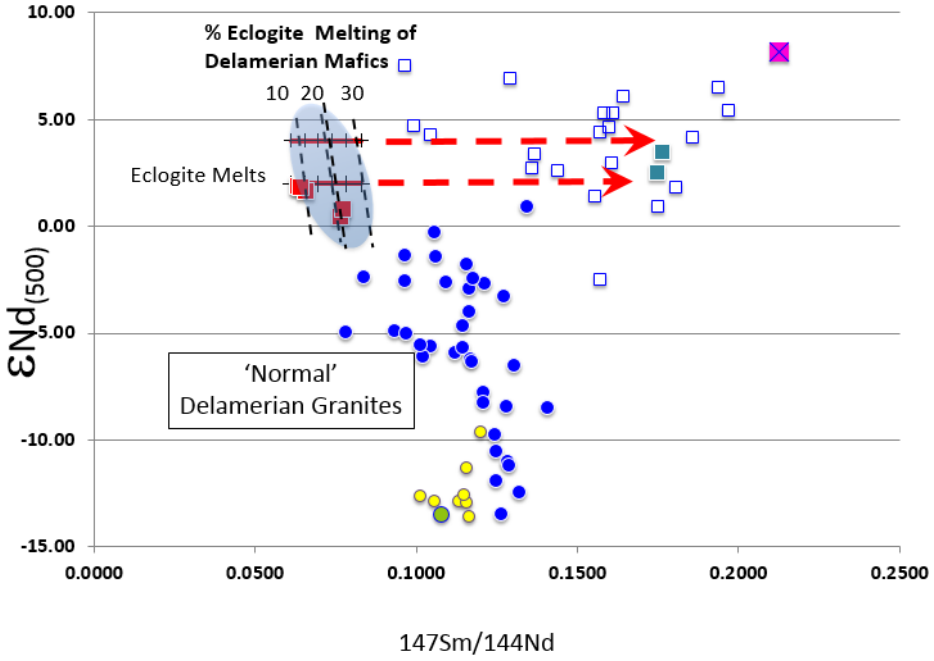

Figure 7a: Percentages of Partial Melting plotted with Kinchina adakites (red squares), Kinchina mafics (filled blue squares), Delamerian mafics (clear squares), Delamerian Granites (blue dots), Kanmantoo group (yellow dots) and Kinchina Migmatite (green circle)

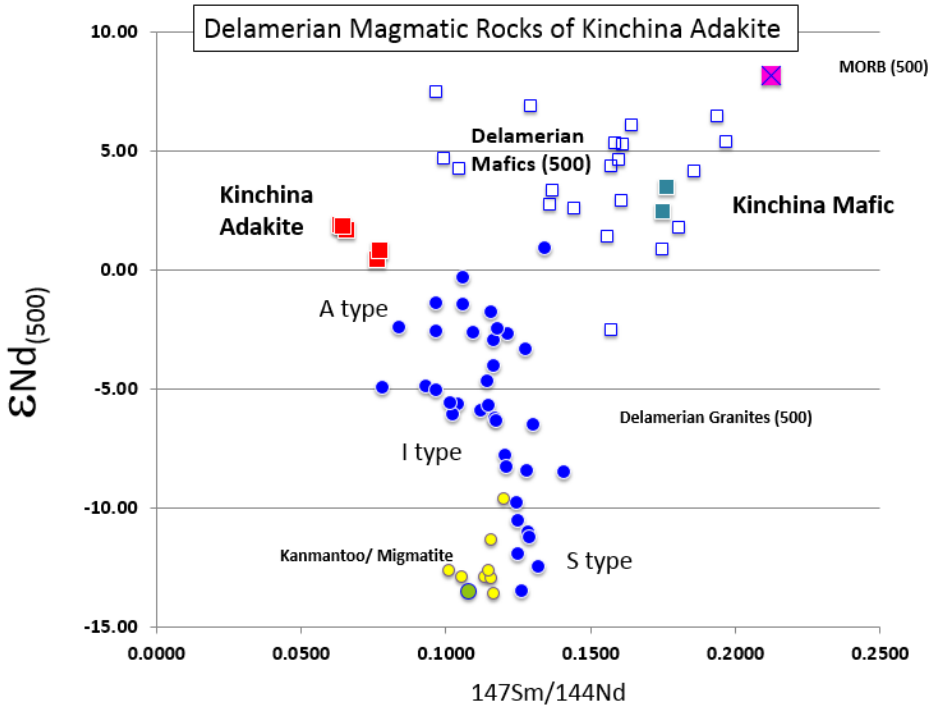

Figure 7b: Epsilon Nd and 147Sm/144Nd of Delamerian Magmatic Rocks of Kinchina adakite including Kinchina mafic plotted against MORB

DISCUSSION

Comparing and contrasting the Kinchina adakite with the surrounding Delamerian granites the differences are clear. The S and I type granites are syn-tectonic with ages between 517-490Ma while the A type are post-tectonic at 485-475Ma. The Kinchina adakite with an age of 495Ma sits with the S and I types as syn-tectonic. In comparing the Kinchina adakites with globally known adakites they share in almost all classification schemes (Table 7) A significant difference being the enrichment in SiO_2, making these adakites like the "high SiO_2 adakites" (Castillo, 2006)

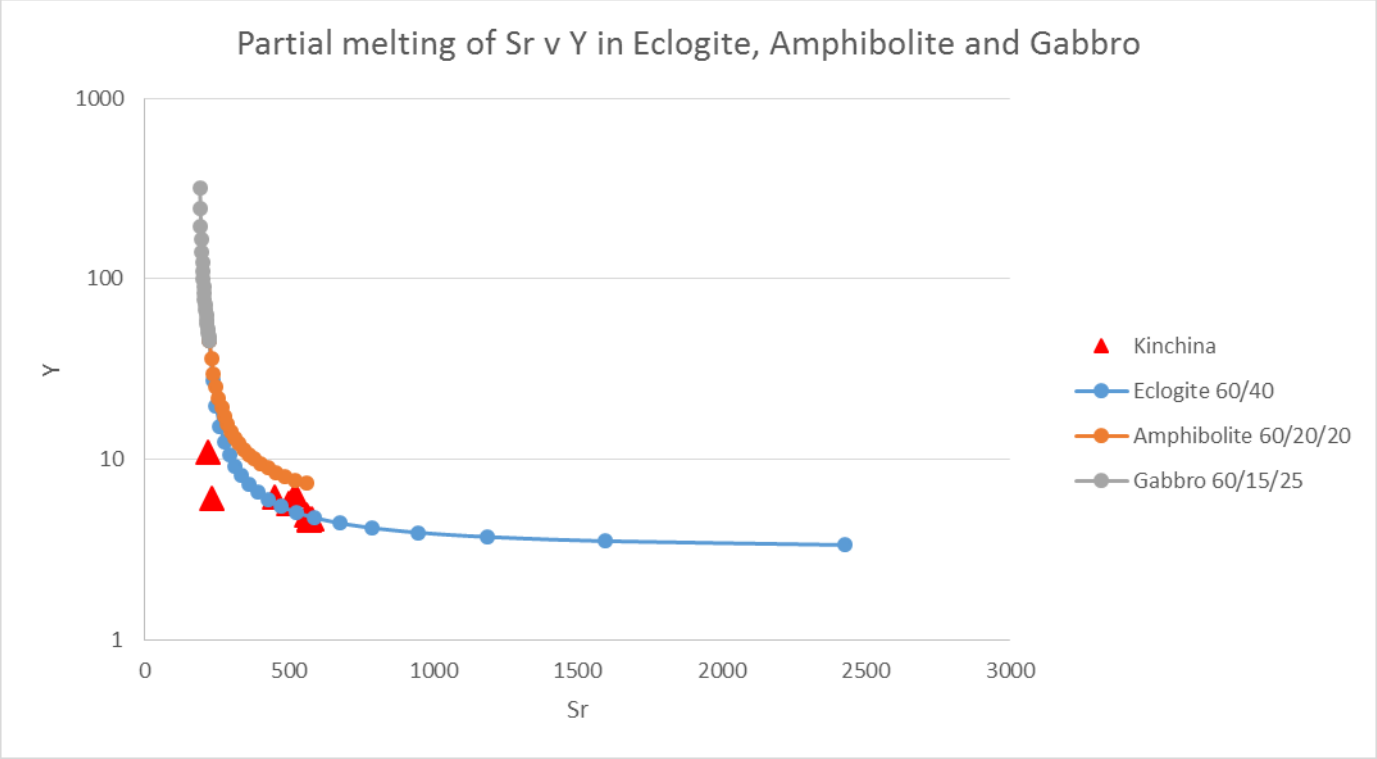

Figure 8a: Sr v Y trace element patterns for different mineral assemblages compared to the adakites

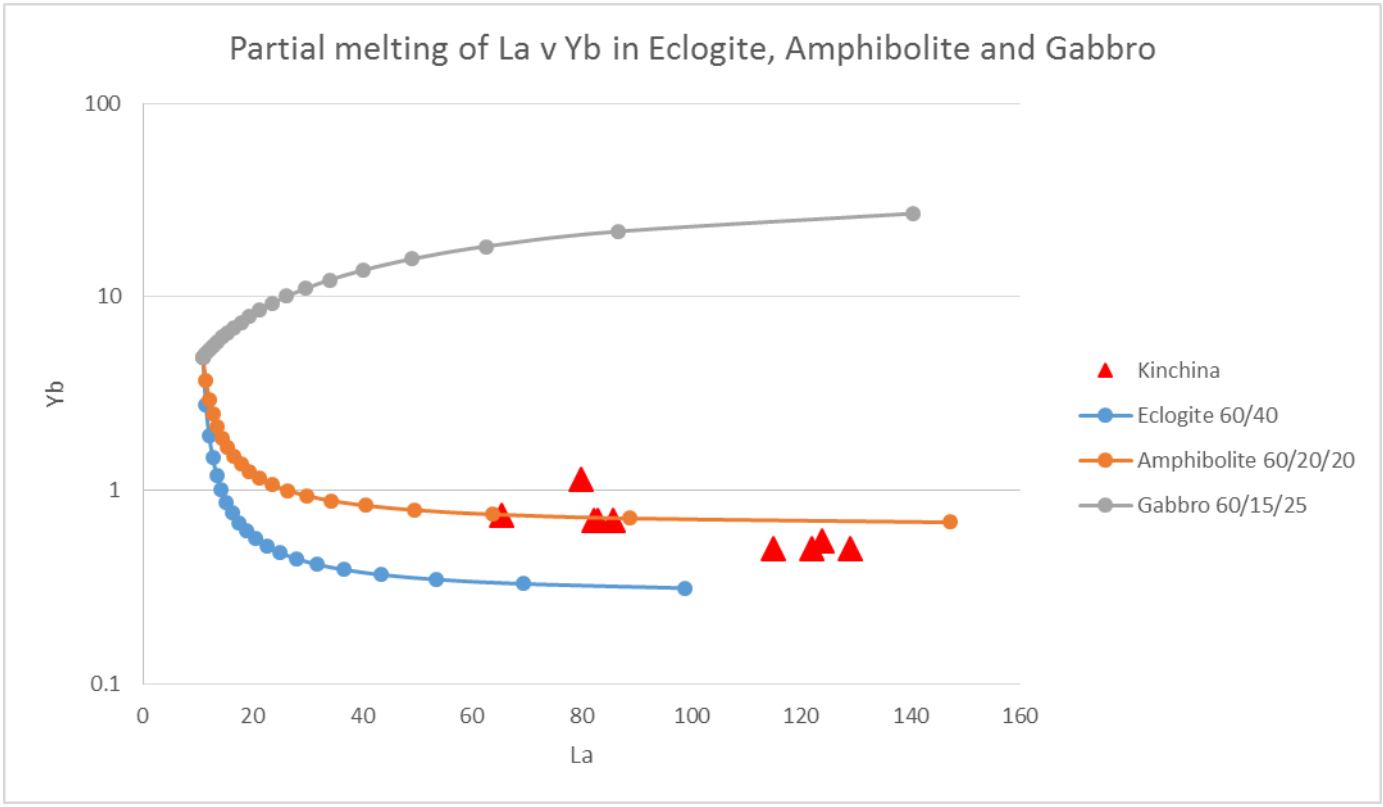

Figure 4b: La v Yb trace element patterns for different mineral assemblages compared to the adakites

In order to determine the most likely partial melting situation an advanced spreadsheet using the partial melting equation (Figure 9), specific distribution coefficients (taken from the GERM website (https://earthref.org/KDD/) with a range of variables including: mineral assemblages (olivine, orthopyroxene, clinopyroxene, garnet, amphibole, plagioclase, spinel and rutile), normalised mineral percentages, bulk distributions, fraction of partial melting, trace element and rare earth elements. All of these variables depended on the percentage of each mineral, this allowed different scenarios to be tested and explored; Figures 8a through to 8b explore these different mineral assemblages. Two trace element pairs (most likely to occur in an adakitic melt) were graphed using different rock types, these included: eclogites with 60% clinopyroxene and 40% garnet, Amphibolite with 60% amphibole, 20% garnet and 20% plagioclase and finally a

gabbro with 60% plagioclase, 25% orthopyroxene and 15% clinopyroxene. Potting the trace elements against each other (eg Sr v Y) and adding in the values from Kinchina samples allowed a comparison to be made between the samples and the best fitting melt scenario. Ultimately, the best scenario through both scenarios is the eclogite with 60% clinopyroxene and 40% garnet. As well as this, the model suggest the mafic source had "seen" the continental crust before being returned to the mantle which suggests delamination and partial melting at P >1.4Gpa and temperatures at approximately 980 degrees Celsius.

$$\frac{C_1}{C_0} = \frac{1}{D + F(1 - P)}$$

Figure 9: Trace element distribution and partial melting equation (Greenland, 1970)

As well as different partial melting scenarios for trace element pairs, rare earth elements were examined for different melting scenarios. The Kinchina mafics were used as the MORB like standard while the average Kinchina adakite displayed a distinctive drop and plateau towards the heavy rare earth elements. As the adakite has evolved over time it has become exposed to numerous sources, ultimately becoming enriched in the light rare earth elements and depleted in the heavy rare earth elements (Figure 4) This depletion in the heavy rare earth elements is due to the presence of garnet as heavy rare earth elements prefer to partition into garnet. A number of different melting scenarios were compared in order to determine the most suitable: which turned out to be a 20% eclogite partial melt with the following mineral assemblage: 60% Clinopyroxene, < 5% Amphibole, 35% Garnet and <5% Rutile.

Two mafics (CG-18-11 and CG-18-29), two adakites (CG-18-6 and CG-18-12), one migmatite (CG-18-28) and a pegmatite (CG-18-19) were analysed. Figures 4 and 5 display the rare earth element trends of MORB in comparison to the Kinchina samples (mafics and adakites) as well as surrounding Delamerian granites (A-type, I-type and S-type) Comparing the average mafic and average adakite from Kinchina with MORB (Figure 4) highlights the difference in mafic, adakite and MORB, the Rare Earth Elements (REE) are steeply fractionated in the adakite. The distinguishing point is the granites' drop in Eu in comparison to the adakites (Figure 5) has a steady decline into the heavy rare earth elements. As well as this, the Delamerian granites display much flatter and higher Heavy Rare Earth Elements (HREE) trends in comparison to the adakites. This negative Eu anomaly found throughout the granites is due to crystallisation of plagioclase as Eu preferentially crystallises in plagioclase. This feature of the granites is a key indicator along with the depletion of the HREE of the difference between adakite and granites.

Comparing the isotopic variables of Epsilon Nd and the ratio of 147Sm/144Nd, the mafics show relatively primitive isotope ratios but are slightly more crustal like than MORB (Figure 7b) The adakite is more mantle like (greater than 0), slightly less than the mafics. This potentially occurred due to a MORB like basalt being contaminated as it entered the crust or the mantle source of the MORB-like basalt was contaminated before melting to produce the Kinchina mafics. As well as this the Kinchina adakites show fairly primitive eNd values (more primitive than all the Delamerian granites) but only a little less than the mafics supporting the theory that these adakites evolved from the Kinchina mafics in two scenarios: 1. In eclogite conditions with crustal

contamination coming later or 2. Contamination of the Kinchina mafic before it was in eclogite conditions. This theory of contamination is further explored in the spider plot of Figure 6, compared with MORB the mafic shows positive spikes in K, Pb and Th while the migmatite mirrors this peaks. These anomalies are consistent between both the migmatite and mafic indicating that with the addition of the Migmatite to MORB this would ultimately create the mafic. This further supports the concept of crustal contamination.

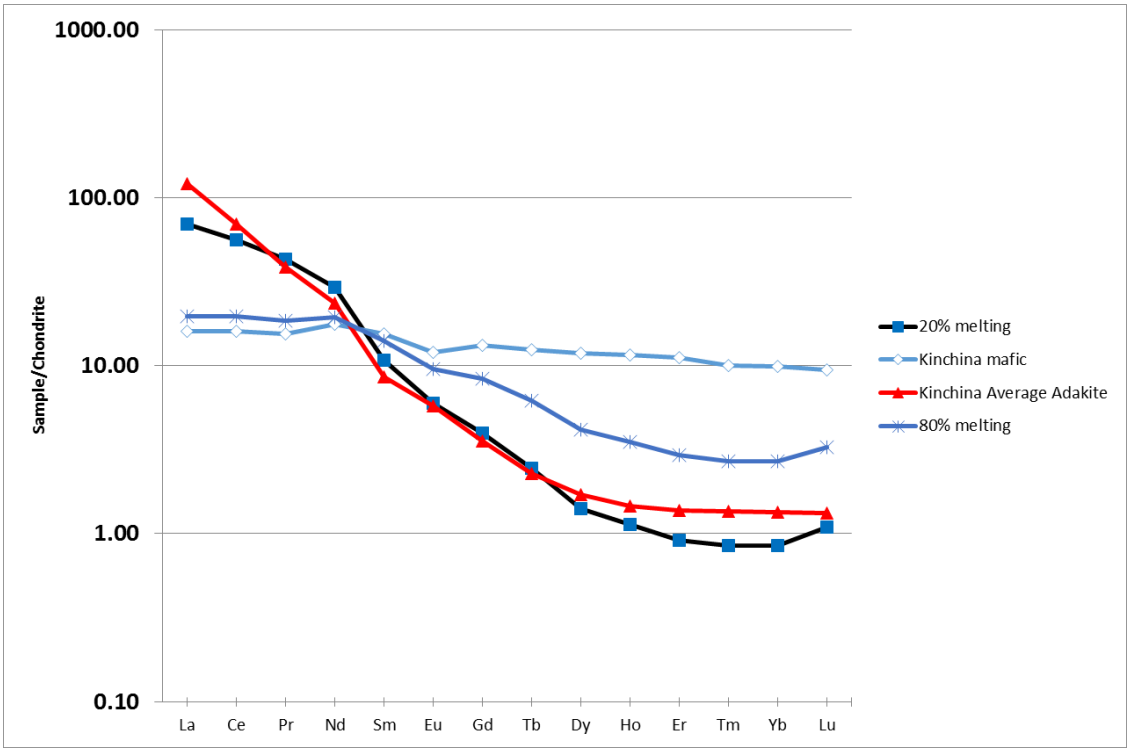

Figure 10: Partial Melting Scenario including Kinchina Average Adakite compared to Kinchina Average Mafic with 20% and 80% partial melting of an Eclogite

Using the same technique as the Trace element partial melting discussed earlier, REE plots were created to best compare the Kinchina average adakite with the Kinchina average mafic REE patterns. Using this Excel spreadsheet, the best model was plotted (Figure 10) and found to be an Eclogite with 20% partial melting; which means the

mafic must have recrystallised to an eclogite facies at about 1.5-3gpa and around 45-80km depth, this suggests delamination. The mafic must have been to the crust, shifted its 147Sm/144Nd (Figure 7b) turned to an appropriate composition to source the adakite which ultimately would have occurred due to the basalt becoming exposed to the crust and falling back down to the mantle to recrystallise through delamination. Linking together this notion of partial melting and crustal contamination, the 147Sm/144Nd is dependent on the amount of melting in the system (as the ratio increases as does the amount of melt) (Figure 7a) The mafics would have been remelted towards the eclogite field (best fit being 20%) which the Kinchina adakites can be found within.

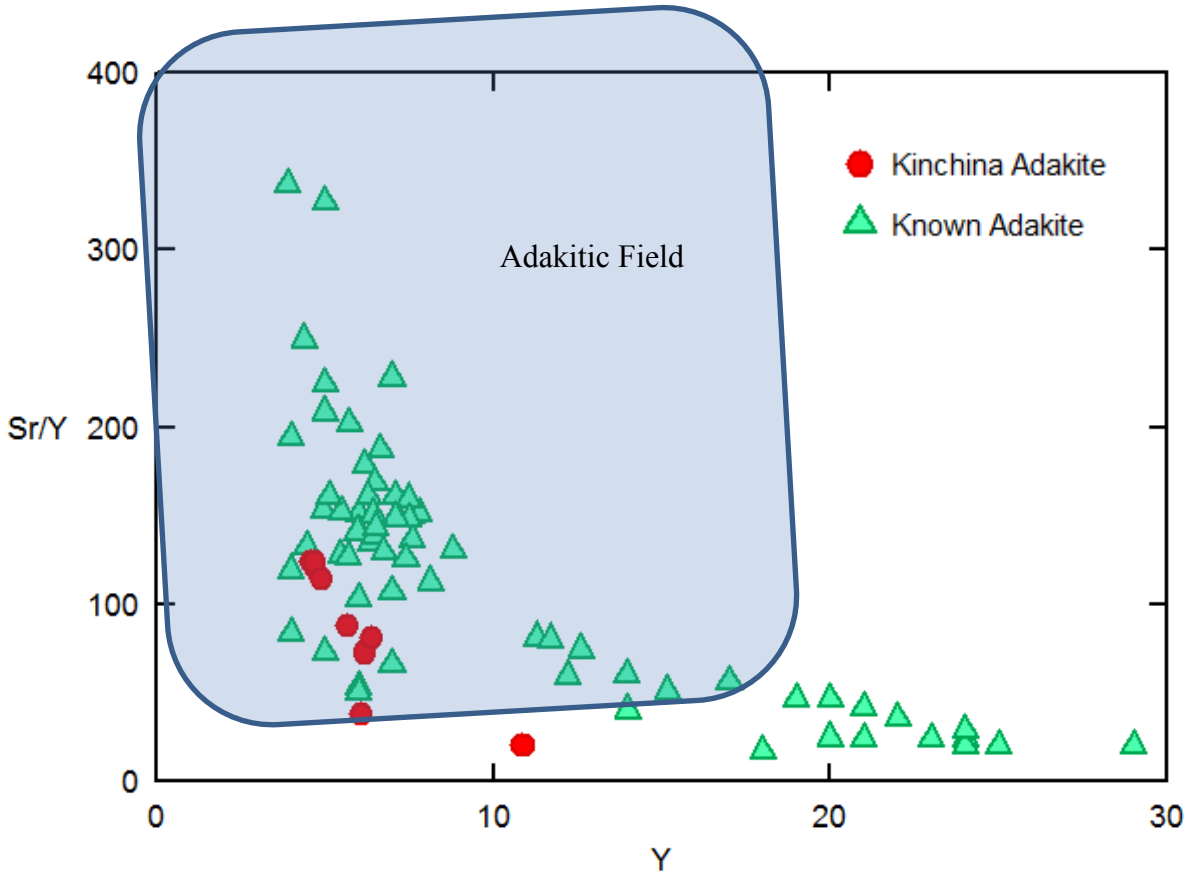

Figure 11: Sr/Y against Y including the adakitic field as presented by (Castillo, 2006) including the Kinchina adakites and known adakites from the literature

Adakites are classified by a very unique set of geochemical characteristics (Table 1) but the most prevalent characteristic throughout the literature is the Sr/Y against Y, which is reflective of garnet and amphibole as residuals. The majority of the Kinchina adakites plot well within the adakite field, again supporting the theory that they are indeed adakites.

Tectonically, the adakites occur at the end of the syn-tectonic phase with the formation of the A-type granites coming shortly after due to upwelling of hot asthenosphere and a thinned lithosphere from the mafic underplate dropping down into the mantle. This sag and drop of the mafic underplate ultimately caused isostatic rebound and exhumation and erosion. This resulted in a back arc basin extending west from the subducting margin in Victoria (approximately 300km to the east)

CONCLUSION

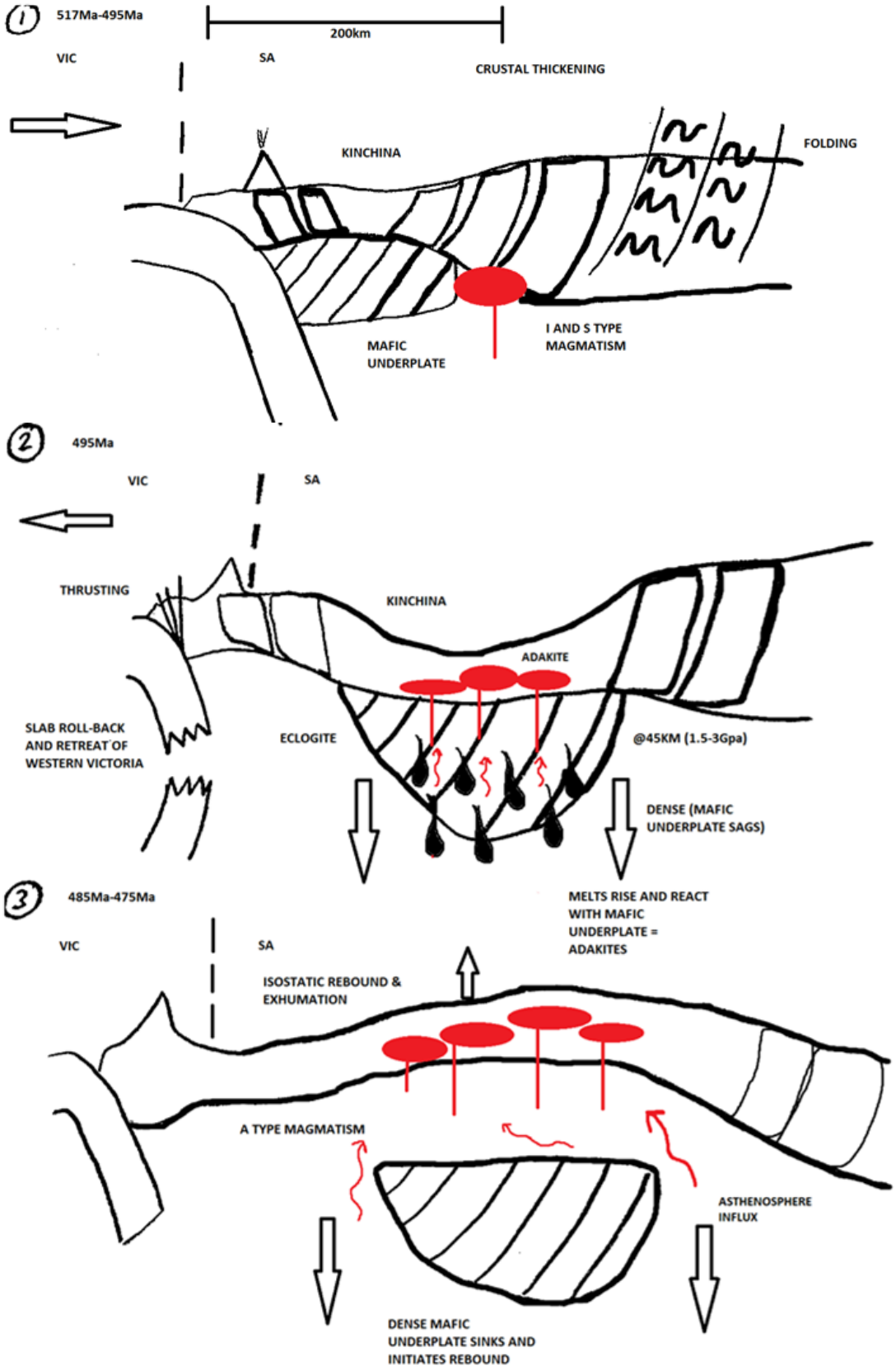

Figure 12: Final concluding sketch of adakite petrogenesis

Following the correct procedures in both the field and laboratories as required, a broad spectrum of data was acquired and finally analysed throughout this paper and project. Considering all data available conclusions can be made regarding the Adakitic rocks of Kinchina and their relationship to Gondwanan subduction.

Characteristics	CG 18 1	CG 18 12	CG 18 6	CG 18 6 Rpt	CG 18 14	CG 18 18	CG 18 2	CG 18 3	CG 18 24
High SiO2 (≥56 wt%)	70.08	71.62	71.82	71.86	71.94	72.67	72.76	72.83	73.12
High Al2O3 (≥15 wt%)	15.5	15.1	15.1	15.1	15.1	14.8	14.6	14.7	14.4
Low MgO (< 3 wt%)	0.66	0.52	0.52	0.53	0.53	0.44	0.43	0.61	0.57
High Sr (>300 ppm)	220	580	570	570	560	520	450	230	500
No Eu anomaly	Yes	Yes	Yes	Yes	Yes	Yes	Yes	Yes	Yes
Low Y (< 15 ppm)	10.9	4.7	4.7	4.6	4.9	6.4	6.2	6.1	5.7
High Sr/Y (>20)	20.1834862	123.4043	121.2766	123.913	114.2857	81.25	72.58065	37.70492	87.7193
Low Yb (<1.9 ppm)	1.15	0.55	0.5	0.5	0.5	0.7	0.7	0.7	0.75
High La/Yb (>20)	69.4782609	225.4545	258	230	244	118.4286	122.4286	117.5714	87.33333

Table 7: Combination of Kinchina adakites and characteristics taken from (Castillo, 2006) summarising the similarities

- The Monarto Granite believed to be an adakite is in fact adakitic in composition (Table 1) and consistent with other geochemical characteristics (Table 7)

- The age of the adakite is 495.37Ma ± 0.58Ma and it is syntectonic with The Delamerian Orogeny.

- The adakite formed due to a hot influx of mantle rising and reacting with a mafic underplate ultimately delaminating (Figure 12), this reaction of heat and mafic underplate combined created a 20% partial melting scenario of an eclogite with

60% Clinopyroxene + 35% Garnet + Amphibole + Rutile. P >1.4Gpa and temperatures at approximately 980 degrees Celsius.

- Due to the isostatic sag of the mafic underplate, this delamination ultimately caused an isostatic rebound and uplift of the Orogeny (Figure 12).

- The Kinchina mafic occurred due to a MORB style melt being contaminated by the Kanmantoo group at crustal pressure in the plagioclase stable field.

ACKNOWLEDGMENTS

This research project would not have been approved or completed without the additional help and feedback provided by: John Foden, Grant Cox, Juraj Farkas, Morgan Blades and Alec Walsh. The data explored and analysed wouldn't be made available without the assistance of Adelaide Microscopy (Sarah Gilbert and David Kelsey), Tom Raimando from Uni SA, and of course David Bruce from the isotope laboratories at The University of Adelaide. I would also like to thank Laura Rollison for assisting with discussions.

REFERENCES

Boger, S., & Miller, J. M. (2004). Terminal suturing of Gondwana and the onset of the Ross–Delamerian Orogeny: the cause and effect of an Early Cambrian reconfiguration of plate motions. *Earth and Planetary Science Letters, 219*(1-2), 35-48.

Castillo, P. R. (2006). An overview of adakite petrogenesis. *Chinese science bulletin, 51*(3), 257-268.

Cox, G. M., Foden, J., & Collins, A. S. (2018). Late Neoproterozoic adakitic magmatism of the eastern Arabian Nubian Shield. *Geoscience Frontiers*.

Defant, M. J., & Drummond, M. S. (1990). Derivation of some modern arc magmas by melting of young subducted lithosphere. *nature, 347*(6294), 662.

Foden, J., Elburg, M. A., Dougherty-Page, J., & Burtt, A. (2006). The timing and duration of the Delamerian Orogeny: correlation with the Ross Orogen and implications for Gondwana assembly. *The Journal of Geology, 114*(2), 189-210.

Foden, J., Elburg, M. A., Turner, S., Sandiford, M., O'Callaghan, J., & Mitchell, S. (2002). Granite production in the Delamerian orogen, South Australia. *Journal of the Geological Society, 159*(5), 557-575.

Foden, J., Song, S. H., Turner, S., Elburg, M., Smith, P., Van der Steldt, B., & Van Penglis, D. (2002). Geochemical evolution of lithospheric mantle beneath SE South Australia. *Chemical Geology, 182*(2), 663-695.

Greenland, L. P. (1970). An equation for trace element distribution during magmatic crystallization. *American Mineralogist: Journal of Earth and Planetary Materials, 55*(3-4_Part_1), 455-465.

Gum, J. (1998). *The sedimentology, sequence stratigraphy and mineralisation of the Silverton Subgroup, South Australia.* University of South Australia.

Macpherson, C. G., Dreher, S. T., & Thirlwall, M. F. (2006). Adakites without slab melting: high pressure differentiation of island arc magma, Mindanao, the Philippines. *Earth and Planetary Science Letters, 243*(3), 581-593.

Moyen, J.-F. (2009). High Sr/Y and La/Yb ratios: the meaning of the "adakitic signature". *Lithos, 112*(3-4), 556-574.

Pawley, M. (2013). A user's guide to migmatites: Geological Survey of South Australia, Resources and Energy Group.

Qian, Q., & Hermann, J. (2013). Partial melting of lower crust at 10–15 kbar: constraints on adakite and TTG formation. *Contributions to Mineralogy and Petrology, 165*(6), 1195-1224.

Richards, J. P., & Kerrich, R. (2007). Special paper: adakite-like rocks: their diverse origins and questionable role in metallogenesis. *Economic geology, 102*(4), 537-576.

Thorkelson, D. J., & Breitsprecher, K. (2005). Partial melting of slab window margins: genesis of adakitic and non-adakitic magmas. *Lithos, 79*(1-2), 25-41.